DEVELOPMENTAL DYNAMICS 242:1262–1283, 2013

RESEARCH ARTICLE

Embryonic Development of Goldfish (*Carassius auratus*): A Model for the Study of Evolutionary Change in Developmental Mechanisms by Artificial Selection

Hsin-Yuan Tsai,[1,2] Mariann Chang,[1] Shih-Chieh Liu,[1] Gembu Abe,[1] and Kinya G. Ota[1]*

Background: Highly divergent morphology among the different goldfish strains (*Carassius auratus*) may make it a suitable model for investigating how artificial selection has altered developmental mechanisms. Here we describe the embryological development of the common goldfish (the single fin *Wakin*), which retains the ancestral morphology of this species. Results: We divided goldfish embryonic development into seven periods consisting of 34 stages, using previously reported developmental indices of zebrafish and goldfish. Although several differences were identified in terms of their yolk size, epiboly process, pigmentation patterns, and development rate, our results indicate that the embryonic features of these two teleost species are highly similar in their overall morphology from the zygote to hatching stage. Conclusions: These results provide an opportunity for further study of the evolutionary relationship between domestication and development, through applying well-established zebrafish molecular biological resources to goldfish embryos. *Developmental Dynamics 242:1262–1283, 2013*. © 2013 Wiley Periodicals, Inc.

Key words: domestication; normal developmental stages; model organisms

Key findings:

- This study provides the first reliable descriptions of normal embryonic stages of wild-type goldfish.
- The embryonic features of goldfish and zebrafish are almost directly comparable.
- Goldfish embryos provide a novel model for the investigation of the evolutionary relationship between domestication and development.

Accepted 16 July 2013

INTRODUCTION

In recent years, the genomic background of divergent morphological features have been intensively studied in domesticated dogs and pigeons, the classic model organisms for the study of evolutionary biology and artificial selection (Lindblad-Toh et al., 2005; Wayne and Ostrander, 2007; Akey et al., 2010; VonHoldt et al., 2010; Stringham et al., 2012; Shapiro et al., 2013). Such investigations have contributed significantly to our understanding of how genes, loci, and alleles were selected for by breeders and fanciers during artificial selection of morphological features (Wayne and Ostrander, 2007; VonHoldt et al., 2010; Akey et al., 2010; Shapiro et al., 2013), while simultaneously prompting researchers to ask how the evolution of developmental mechanisms and artificial selection are related (Morey, 1994; Trut et al., 2009; see also Gilbert, 2010). To address this question, it is important to identify additional model organisms with the following properties: established morphologically divergent strains, as seen for dogs and pigeons (Lindblad-Toh et al., 2005; Wayne and Ostrander,

[1]Laboratory of Aquatic Zoology, Marine Research Station, Institute of Cellular and Organismic Biology, Academia Sinica, Yilan, Taiwan
[2]The Roslin Institute and Royal (Dick) School of Veterinary Studies, University of Edinburgh, Midlothian, United Kingdom
Grant sponsor: The National Science Council of Taiwan; Grant number: 102-2313-B-001-005-MY3.
***Correspondence to: Kinya G. Ota, Laboratory of Aquatic Zoology, Marine Research Station, Institute of Cellular and Organismic Biology, Academia Sinica, No.23-10, Dawen Road, Jiaoxi, Yilan, 26242, Taiwan. E-mail: otakinya@gate.sinica.edu.tw**

DOI: 10.1002/dvdy.24022
Published online 31 July 2013 in Wiley Online Library (wileyonlinelibrary.com).

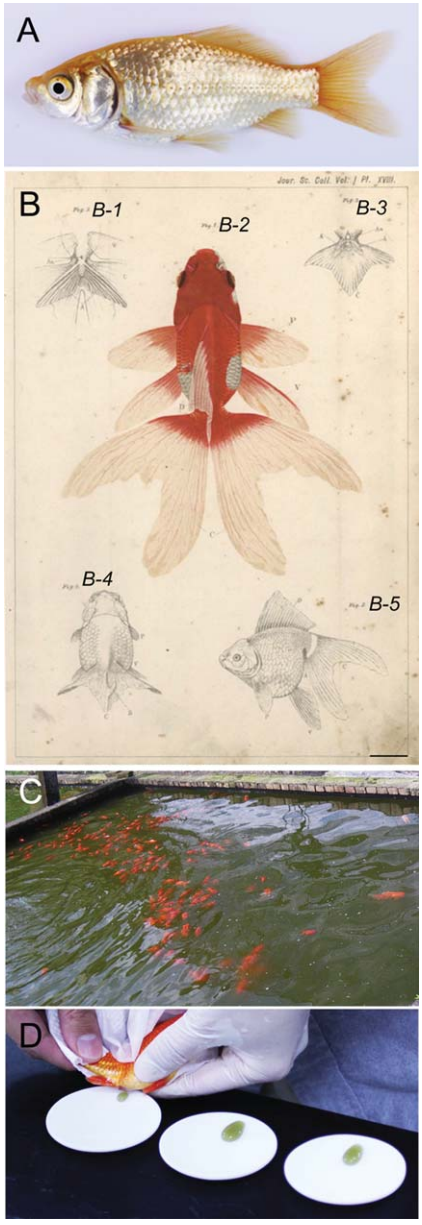

Fig. 1. Adult goldfish specimens. **A:** Lateral view of the common goldfish (the single fin *Wakin*) strain. **B:** Illustrations of two goldfish strains by Watase (1887). B-1: Ventral view of the bifurcated anal fin of *Ryukin* strain. B-2: Dorsal view of *Ryukin* strain. B-3, 4: Ventral and dorsal views of *Ranchu* strain; the dorsal fin is absent in this strain. B-5: Lateral view of the *Ryukin* strain. **C:** A pond with several goldfish in Taiwan. **D:** Artificially squeezed goldfish eggs on Teflon dishes. Approximately 500 to 1,000 eggs can be obtained from a single female (approximately 10 cm in length).

2007; Akey et al., 2010; VonHoldt et al., 2010; Stringham et al., 2012; Shapiro et al., 2013); and ease of handling and observation of embryos, such as for zebrafish and medaka (Kimmel et al., 1995; Takeda and Shimada, 2010).

The goldfish (*Carassius auratus*) is a well-known domesticated species (Fig. 1). According to analyses of Chinese archives, breeding of this teleost fish as an ornamental animal dates back around 1,000 years ago (Chen, 1925, 1956; Smartt, 2001).

During its domestication, several strains have been isolated and genetically fixed in the goldfish population by breeders and fanciers (Matsui and Axelrod, 1991; Smartt, 2001; Komiyama et al., 2009). Although there is no standardized classification method (Matsui and Axelrod, 1991; Smartt, 2001), one textbook categorized modern goldfish strains into 16 groups, based on the trunk shape, eye morphology, coloration, and the number and length of the fins (see Smartt, 2001; Fig. 1).

These morphological varieties of goldfish strains support the conceptual understanding of divergent morphological features, originally proposed by 19th century biologists (Darwin, 1868; Bateson, 1894). Based on its historical background and morphological features, goldfish may be a suitable model organism for the study of artificial selection, along with domesticated dogs and pigeons (Lindblad-Toh et al., 2005; Wayne and Ostrander, 2007; Akey et al., 2010; VonHoldt et al., 2010; Stringham et al., 2012; Shapiro et al., 2013). Moreover, because goldfish are commercially available and a large number of eggs can be obtained from a single female (Fig. 1C,D), goldfish embryos have been used for studies of developmental biology (Yamaha et al., 1998, 1999, 2001, 2002, 2003; Mizuno et al., 1997, 1999; Otani et al., 2002; Tanaka et al., 2004).

These reports indicate that goldfish have the above mentioned properties required for the investigation of evolutionary change of developmental mechanisms by artificial selection. In addition, goldfish are phylogenetically closely related to zebrafish (Saitoh et al., 2003, 2006; Komiyama et al., 2009). Indeed, certain molecular developmental studies of goldfish embryos used zebrafish techniques, which enabled investigation of germ cell lineage and retinal development (Passini et al., 1997; Otani et al., 2002; Chen et al., 2009). These reports suggest that the developmental processes of these organisms may be comparable, enabling molecular developmental studies in goldfish with reference to existent zebrafish data and tools, including mutants, morphants, and gene expression patterns, recorded in "The Zebrafish Model Organism Database" (Bradford et al., 2011). However, our knowledge remains insufficient to compare zebrafish and goldfish embryos, on account of a lack of reliable developmental descriptions of wild-type goldfish, the morphology of which resembles the ancestral state (Matsui, 1934; Smartt, 2001).

Previous publications have reported on the developmental processes of goldfish (Watase, 1887; Khan, 1929; Battle, 1940; Harvey and Hems, 1948; Li et al., 1959; Kajishima, 1960; Sharma and Ungar, 1980; Yamaha et al., 1999; Nagai et al., 2001; Otani et al., 2002; see also Smartt, 2001). Three of these researchers provided detailed descriptions of embryonic development and staging tables (Li et al., 1959; Kajishima, 1960; Yamaha et al., 1999) (Table 1). Two early goldfish staging tables, by Li et al. (1959) and Kajishima (1960), covered different embryonic stages from fertilization to hatching. A comparative staging table between goldfish and zebrafish was subsequently published (Yamaha et al., 1999), but its covering stage is limited to the early embryonic stages (from zygote to mid-gastrulation). Moreover, the identity of the goldfish strains used for the observation of development in these studies are not entirely clear (Li et al., 1959; Kajishima, 1960; Yamaha et al., 1999); it is possible that some of these staging tables contain mixed embryonic descriptions of wild-type and morphologically divergent strains. In fact, there is no specific description of the morphological traits of the goldfish strains used to generate the staging table of Yamaha et al. (1999). Moreover, although Li et al. (1959) and Kajishima (1960) mentioned that several different strains were used for the embryological observations, the strains used for recording the developmental stages were not specified. As such, the previously generated staging tables may be promiscuous, in that they are derived from multiple goldfish strains. Consequently, there is essentially no wild-type goldfish staging table that is comparable with

TABLE 1. Comparison of Published Staging Schemes of Goldfish

Kimmel et al., 1995 Zebrafish (28.5°C)	Yamaha et al., 1999 (20°C)	Kajishima 1960 (21±1°C)	Li et al., 1959 (25°C)
Zygote period			
1-cell (0h)	1-cell (0h)	Fertilized egg (30min)	1-cell (0.73h)
Cleavage period			
2-cell (0.75h)	2-cell (1h)	2-cell stage (1 h)	2-cell (0.9h)
4-cell (1h)	4-cell (1.5h)	4-cell stage (1.5h)	4-cell (1.19h)
8-cell (1.25h)	8-cell (2h)	8-cell stage (2h)	8-cell (1.40h)
16-cell (1.5h)	16-cell (2.5h)	16-cell stage (2.5h)	16-cell (1.75h)
32-cell (1.75h)	32-cell (3h)	32-cell stage (3h)	32-cell (2.03h)
64-cell (2h)	64-cell (3.5h)	Morula stage (3.5h)	64-cell (2.33h)
Blastula period			
128-cell (2.25h)	128-cell (4h)		Early high blastula (2.64h)
256-cell (2.5h)	256-cell (4.75h)		Late high blastula (3.35h)
512-cell (2.75h)	512-cell (5.7h)		Flat blastula (3.84h)
1k-cell (3h)			Early gastrula (6.13h)
High (3.3h)	Mixing (8h)	High blastula (4h)	
Oblong (3.6h)	Yolk syncytial layer formed (9.5h)		
Sphere (4h)			
Done (4.3h)		Flat blastula (5.5h)	
30%-epiboly (4.6h)	30%-epiboly (11h)	Expanding blastula (7h)	
Gastrula period			
50%-epiboly (5.25h)			Middle gastrula (7.45h)
Germ-ring (5.6h)	Germ-ring (13.3)		
Shield (6h)	Embryonic Shield (15h)	Early gastrula (9.5h)	
75%-epiboly (8h)		Middle gastrula (11h)	
90%-epiboly (9h)		Late gastrula (13h)	Late gastrula (9.87h)
Bud (10h)		Early embryonic shield (15h)	Blastopore closure (11.39h)
		Late embryonic shield (18h)	
Segmentation period			
1-somite (10.3h)			
5-somite (11.6h)		Optocole develops (21h)	Fore brain formation/3–5somite (14.47h)
14-somite (16h)		Optic vesicle develops (26h)	optic vesicle formation/6–14 somite (15.75h)
			Hind brain formation/15–16 somite (19.68h)
			nasal capsule formation/17–19 somite (20.53h)
20-somite (19h)		Optic cup and lens development (30h)	
			Lens formation/20–21 somite (22.42h)
			Central nervous system tube formation/22–23 somite (22.93h)
			Mid brain formation/24 somite (23.67h)
			Heat beat/25 somite (25.50h)
26-somite (22h)		Tail bud stage (33h)	Otolith formation/26–27somite (26.41h)
Pharyngula period			
Prim-5 (24h)		Retinal pigmentation begins (36h)	
Prim-15 (30h)		Melanophores first appear on embryo (50h)	Circulation/35somite (30.62h)
Prim-25 (36h)		Heart pulsates, and circulation begins (60h)	
High-pec (42h)		Pectoral fin bud appears (80h)	Coelom formation/Pectoral limb bud (31.64h)
Hatching period			
Long-pec (48h)		Hatching (100 h)	Major vein formation/Pigmentation (33.04h)
			Caudal median fin fold formation (34.53h)
Pec-fin (60h)			Fin ray formation (38.01h)
Protruding-mouth (72h)			Hatch out (64.93h)

the normal developmental stages of zebrafish (Kimmel et al., 1995).

Therefore, we describe here the developmental processes of the common goldfish (the single tail *Wakin*, which has highly similar morphology to the wild-type; Fig. 1A) (Matsui and Axelrod, 1991; Smartt, 2001) from fertilization to hatching, referencing the zebrafish staging table. Our present observations indicate that the embryos of zebrafish and goldfish are highly similar in terms of embryonic morphology, suggesting that mutant goldfish and zebrafish can be compared by their phenotypes. Such similarity also suggests that the established techniques and knowledge of zebrafish molecular developmental biology may be directly applicable to goldfish embryos, throughout development.

RESULTS

General Description

Male and female goldfish with no morphological mutations (generally referred to as common goldfish) were purchased from an aquarium shop in Taiwan (Fig. 1A) (see Experimental Procedures). Fertilized eggs were obtained by artificial fertilization, spread onto plastic dishes, and incubated at 24°C. To confirm that embryos derived from the common goldfish parents retained their phenotype, the morphological features of more than 50 hatched embryos of each cross were examined under light microscopy.

Developmental stages are summarized in Table 2. These stages are categorized into seven periods (Zygote, Cleavage, Blastula, Gastrula, Segmentation, Pharyngula, and Hatching periods) based on the zebrafish staging table (Kimmel et al., 1995). The goldfish zygote, cleavage, blastula, gastrula, and segmentation periods were relatively easily defined by using the indices of the zebrafish developmental staging system (Kimmel et al., 1995). However, the stage corresponding to the zebrafish pharyngula period was less apparent, as staging based on the position of the lateral line primordia could not be directly applied to goldfish embryos (Kimmel et al., 1995). Thus, we redefined the stages in this period, categorizing them into three stages (see below). Moreover, the high-pec stage was not used as we were unable to define it in goldfish embryos (Table 2).

The relationship between the stages and time after fertilization at 24°C are also presented in Table 2. We succeeded in collecting a large number of sampling points from the zygote to the segmentation period (208 points in total), to analyze the developmental rate (Fig. 2). In the goldfish embryos, hours post fertilization (hpf) showed a linear correlation with the developmental stages in the cleavage, blastula, and segmentation periods (Fig. 2). In addition, the developmental rate of these goldfish embryonic stages was largely consistent with previous reports (Li et al., 1959; Kajishima, 1960; Yamaha et al., 1999) (Fig. 2). These results suggest that our goldfish staging table is reliable for these three periods (Table 2; Fig. 2). However, we could not obtain accurate data for the gastrula period, due to difficulties in applying the zebrafish staging system (Kimmel et al., 1995) (see below for details). Moreover, in the pharyngula and hatching period, the developmental rate fluctuated dramatically between batches and individual embryos. These fluctuations seem to derive from the condition of female individuals, the timing of egg laying, and handling during the observation process at early embryonic stages. Of particular note, frequent opening and closing of the incubator for embryo observation is highly likely to have resulted in temperature changes in the incubation chamber. In fact, the embryos which were used for observing early stages showed extreme fluctuations in developmental rate at late stages. To avoid, or at least minimize, artifacts from handling, we prepared goldfish embryos for observation of late stages only, and re-sampled a few late stage embryos (31 points; plotted as black circles in Fig. 3). Based on these re-sampled late stage embryos, we estimated an approximate developmental rate, for which the estimated time of hatching is largely consistent with that reported by Li et al., (1959) (Table 2; Fig. 3).

Zygote, Cleavage, and Blastula periods

These periods were previously observed by three authors independently, and the morphological descriptions and developmental rates are generally similar (Li et al., 1959; Kajishima, 1960; Yamaha et al., 1999) (Table 2). Moreover, relatively convincing and reliable descriptions have also been reported (Yamaha and Yamazaki, 1993; Yamaha et al., 1998, 1999, 2001, 2002, 2003; Mizuno et al., 1997, 1999; Nagai et al., 2001; Otani et al., 2002; Tanaka et al., 2004). As such, we only provide brief descriptions of the developmental process, and goldfish-specific features in these embryonic periods, for comparison with earlier reports (Li et al., 1959; Kajishima, 1960; Yamaha et al., 1999) (Figs. 4–6).

One-cell stage

After goldfish eggs are exposed to water, their perivitelline space appears, and their chorion develops strong adhesiveness to the substrate (Fig. 4A). The eggs do not easily detach from the substrate, and eggs will occasionally attach to one another (Fig. 4A). On account of its thickness and adhesiveness, the surface of the goldfish chorion appears white under the microscope, and its transparency is lower than zebrafish eggs, especially at this stage (Fig. 4B).

Cleavage period (2-cell to 64-cell stage)

We defined the cleavage period as consisting of six stages: 2-, 4-, 8-, 16-, 32-, and 64-cell stages (Fig. 5). Cleavage in fertilized goldfish eggs is meroblastic, as in other teleost fishes (Swarup, 1958; Armstrong and Child, 1965; Benzie, 1968; Ballard, 1973; Kimmel et al., 1995; Martinez and Bolker, 2003; Iwamatsu, 2004; Hall et al., 2004; Fujimoto et al., 2004; Fujimura and Okada, 2007; Hinaux et al., 2007). The first cleavage of the blastodisc cytoplasm takes around 40 min postfertilization at 24°C, and forms two equal-sized blastoderms (Figs. 2, 5A). Subsequent cleavages occur every 25 to 30 min during this period (Table 2; Figs. 2, 5B–H). The vertically orientated furrow cleaves the blastodisc up to the 32-cell stage (Fig. 5B–G). The size and shape of the blastoderm cells are almost equal at the 4-cell stage (Fig. 5B). From the 8-cell

TABLE 2. Stages of Embryonic Development

Period	Stage	hpf (24°C)[a]	Descriptions
Zygote period			
	1-cell	0	Perivitelline space appears; cytoplasm moves to animal pole to form the blastodisc
Cleavage period			
	2-cell	0.4	Partial cleavage
	4-cell	0.85	2x2 array of blastomeres
	8-cell	1.3	2x4 array of blastomeres
	16-cell	1.75	4x4 array of blastomeres
	32-cell	2.2	1–2 blastomeres layer(s)
	64-cell	2.65	3 blastomeres layers
Blastula period			
	128-cell	3.1	5 blastomere layers
	256-cell	3.55	7–8 blastomere layers
	512-cell	4	9–10 blastomere layers
	1k-cell	4.45	11 blastomere layers
	High	4.9	>11 blastomere layers; beginning of blastodisc flattening and smoothing; an elliptical shape
	Oblong	5.35	Smooth border between blastdisc and yolk; shape remains elliptical
	Sphere	5.8	Spherical or highly compressed pear-shape
	Dome	6.25	Yolk cell doming toward animal pole as epiboly begins
	30%-epiboly	6.7	Blastoderm shows an inverted cup shape; one edge of cup is thinner than the other; margin reaches 30% of distance between the animal and vegetal poles
Gastrula period			
	50%-epiboly	8	Blastoderm shows uniform thickness; margin of blastomere reaches 50% of distance between the animal and vegetal poles
	Germ-ring	8.5	Germ ring visible from animal pole; 50% epiboly
	Shield	8.6	Embryonic shield visible, showing thicker dorsal side
	60%-epiboly	9	Dorsal side distinctly thicker; 25–30% blastopore closure
	90%-epiboly	11	Brain rudiment thickened; tail bud prominent; 70–80% blastopore closure
	95%-epiboly	11.5	Early polster; 85–90% blastopore closure
	Bud	12	Distinctly larger polster and tail bud; 100%-epiboly
Segmentation			
	6-somite	14	Optic primordium begins to show
	10-somite	16	Neuromeres appear
	14-somite	18	Distinct Kupffer's vesicles; v-shaped trunk somites
	18-somite	20	Distinctive yolk extension in the caudal region
	22-somite	22	Muscular twitches; lens and otic vesicles; tail well extended, sculptured brain
Pharyngula period			
	25% OVC	26	Early pigmentation in retina and skin; red blood cells on yolk; median fin fold; heart beat; pectoral fin bud appearance
	35% OVC	35	Retina pigmented strongly; strong heat beat; actinotrichia extension at median fin fold; Equivalent with prim >12 stages
	65% OVC	44	Broad median fin fold with well extended actinotrichia; strongly pigmented ventral side of tail; asymmetric pectoral fin bud; yolk extension beginning to taper; prim >24 stage
Hatching Period			
	Long-pec	58	Distinct yellow colored head; distinctive pre-cloacal fin fold; pectoral fin pointed; head lifting up to dorsal; HTA, 40°
	Pec-fin	64	Pectoral fin flattened fin shape; Dorsal body as yellow as head; HTA, 30°
	Protruding-mouth	72	Wide open mouth protruding anterior; well-developed pre-cloacal median fin fold; slender yolk; distinctly broader caudal fin fold; HTA, 20°

[a]Hours post fertilization (hpf) of gastrula, pharyngula, and hatching period are approximate.

stage, the cells gradually diverge in size and shape, based on their location within the blastoderm (Fig. 5D–H). From the 32-cell stage, blastodermal cells begin to form a three-dimensional formation, with vertically elongated shapes (Fig. 5G). After dividing to form the 64-cell stage, the blastoderm has three layers when viewed from the side (Fig. 5H).

Blastula period (128-cells; 30%-epiboly stage)

Based on the description of zebrafish embryos in this period (Kimmel et al., 1995), the blastula period of goldfish

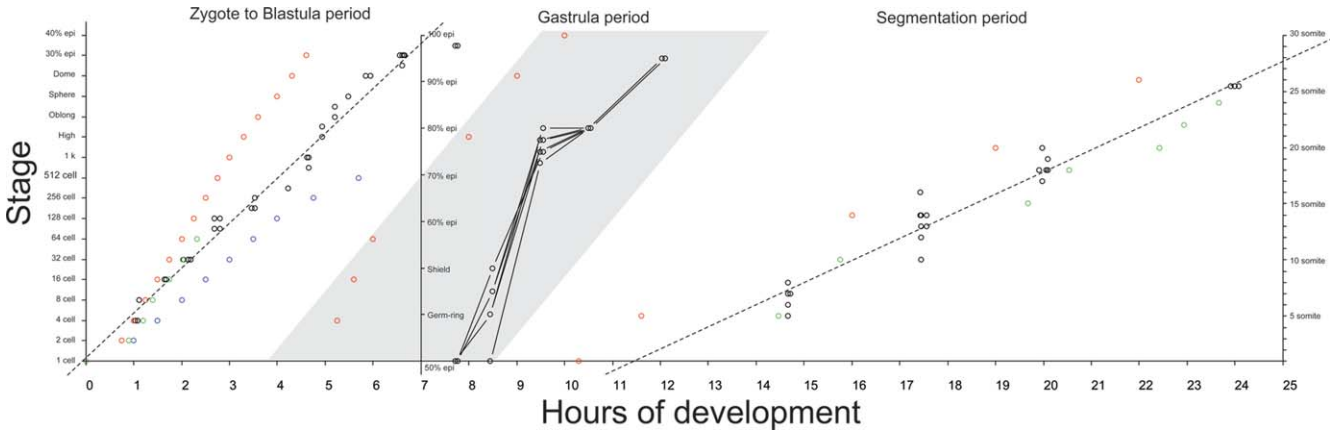

Fig. 2. Rates of development for embryos from the zygote to the segmentation period. Plots of the gastrula period are shaded in gray. The goldfish data are sampled from 208 points, consisting of 119 points from the zygote to the blastula period, 41 points from the gastrula period, and 48 points from the segmentation period. Black open circles indicate the ratio plot between developmental stages and hours post fertilization (hpf). Red, green, and blue open circles indicate the rate of development of zebrafish embryos incubated at 28.5°C (Kimmel et al., 1995), and goldfish embryos incubated at 25°C (Li et al., 1959) and at 20°C (Yamaha et al., 1999), respectively. The dashed lines indicate the linear regressions for goldfish plots of blastula and segmentation periods. The developmental rate in the gastrula periods is represented by the line plots; more than three plots derived from the same embryo are connected by solid lines.

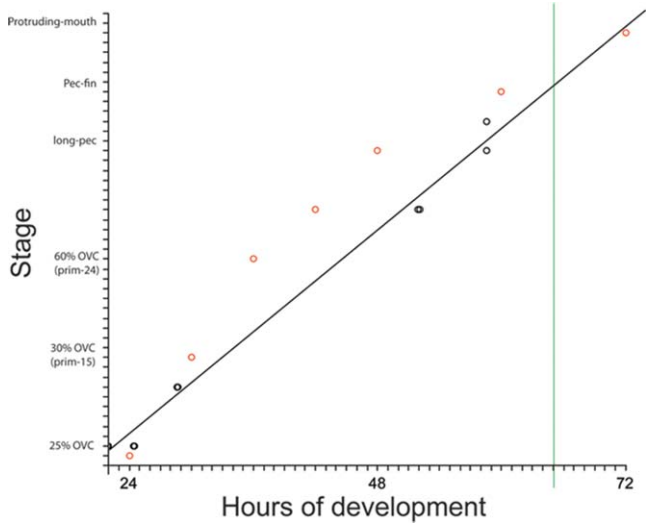

Fig. 3. Rates of development for embryos from the pharyngeal to the hatching period. Black circles plot the ratio between the developmental stages and hours post fertilization (hpf). Red open circles indicate the rate of development for zebrafish at 28.5°C, as in Fig. 2. The vertical green bar indicates the hatching time of goldfish incubated at 25°C (Li et al., 1959). The dashed line indicates the linear regression for the goldfish data in the present study. There are a total of 31 sampling points. These points are distributed at six positions, and thus overlap.

embryos was divided into nine stages, as follows; 128-, 256-, 512-, 1k, high, oblong, sphere, dome, and 30%-epiboly stages (Fig. 6). The blastoderm forms a hemisphere, and 128-cell blastomeres are arranged into a three-dimensional high mound of cells. The surface of the blastoderm is smoother than that at previous stages (Fig. 6A). From the 128-cell to the 1k stage, the boundary between the blastodisc and the yolk has similar features, with a clear contour (Fig. 6B–E). To distinguish between these stages, the number of blastodermal cell layers can be used as an index (Table 2) (Fig. 6A–E).

Although this period of goldfish development has been investigated by Yamaha and colleagues, the descriptions of the 1k to the dome stage were inconsistent (Yamaha et al., 1999, 2001; Otani et al., 2002). Previous reports suggest that the embryos of goldfish are different with those of zebrafish in that the yolk of goldfish is larger; as a result, the high to dome stages are not clearly distinguishable in goldfish embryos (Yamaha et al., 1999). However, we were able to distinguish these stages under darkfield microscopy, by focusing on the appearance of the blastoderm region and its boundary with the yolk (Fig. 6E–H). Moreover, histological analysis of blastula period embryos revealed that the yolk syncytial layer is similar between goldfish and zebrafish (Fig. 7) (see below). The rate of development during this period is 25 to 30 minutes (lasting until the dome stage), and embryos enter the 30%-epiboly stage after a duration exceeding 30 min (Fig. 2).

The shape of the boundary between the blastoderm and the yolk becomes smoother at the high stage (Fig. 6E), and is almost unrecognizable by the oblong stage (Fig. 6F). This smooth boundary between the blastoderm and the yolk was confirmed at the histological level (Fig. 7B). As observed in high-stage zebrafish embryos (Kimmel et al., 1995; Rohde and Heisenberg, 2007; Carvalho and Heisenberg, 2010), the yolk syncytial layer forms a thin ring with a smooth outer edge (Fig. 7).

The yolk outline is compressed at the sphere stage, as compared to the oblong stage (Fig. 6F). The overall shape of the embryo at the high and

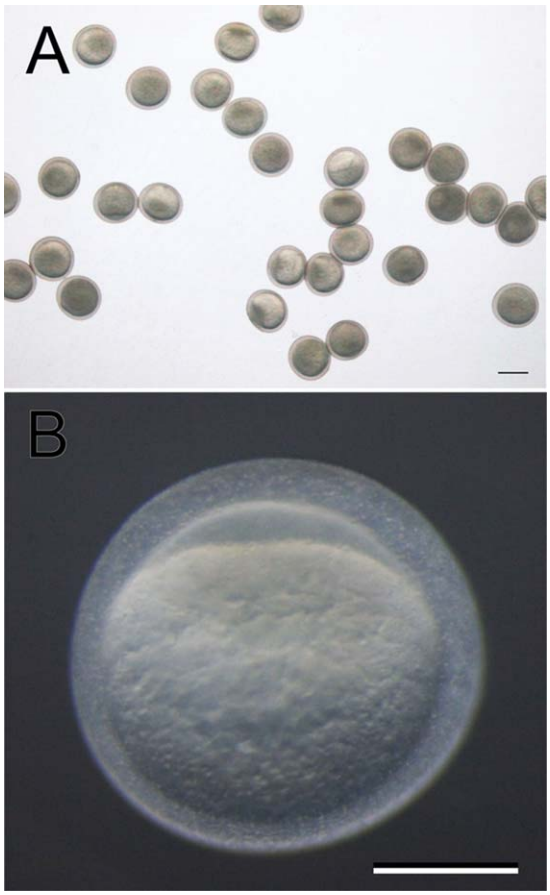

Fig. 4. Zygote stage of goldfish embryos. **A:** Goldfish embryos spread on a plastic dish. Some goldfish embryos are attached to each other. **B:** Side view of a fertilized goldfish egg.

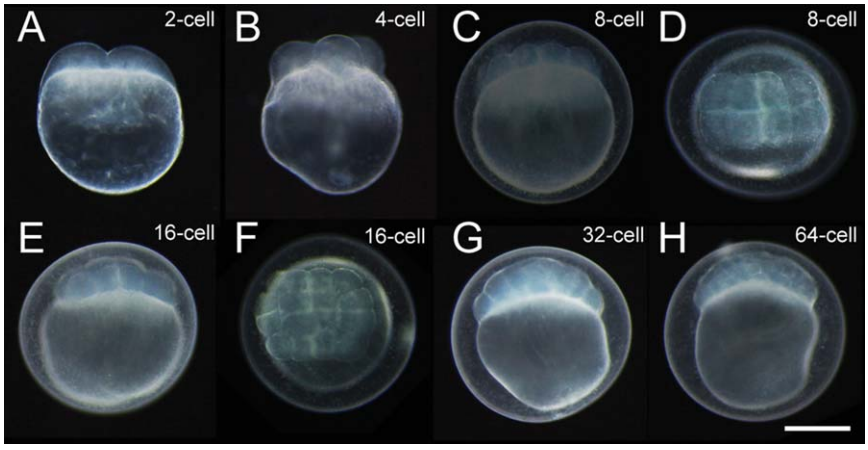

Fig. 5. **A–H**: Cleavage stages of goldfish embryos. A,B: Two-cell and four-cell stage embryos were dechorionated. All panels show a side view, with the exception of panels D and F (animal pole views of 8- and 16-cell stage embryos, respectively). Scale bar = 0.5 mm.

oblong stages is slightly elongated along the animal–vegetal axis, and by the sphere stage, the outline is a "compressed pear shape" (Fig. 6G); this is contrary to zebrafish embryos at the equivalent stage, which are more spherical (Kimmel et al., 1995).

The prominent yolk, the "dome", can be observed in goldfish embryos as well as in zebrafish embryos (Fig. 6H). The dome-like structure is more visible in later stage embryos, of around the 30%-epiboly stage (Fig. 6I). In some goldfish embryos, a dome-like structure can be observed at the oblong stage. However, the goldfish dome and oblong stages can still be distinguished relatively easily based on the shape of the internal blastoderm margin; the outline of the internal blastoderm margin of the dome stage is more highly curved than that of the oblong stage (white arrowhead and arrow in Fig. 6F,H).

Gastrula Period

Based on the indices of zebrafish embryos in this period, goldfish embryos can be categorized into seven stages (50%-epiboly, germ ring, shield, 60%-, 90%-, and 95%-epiboly, and bud stages) (Fig. 8). Although percent-epiboly was used for staging of the zebrafish embryo due to its constancy (Kimmel et al., 1995), it is difficult to apply the same index to goldfish embryos; difficulties arise from the softer and larger yolk of goldfish as compared to zebrafish, and the variance in yolk size between individual goldfish embryos. In fact, although it has been reported that the rate of advance of the blastoderm margin over the yolk shows a linear increase after the 50%-epiboly stage in zebrafish (Kimmel et al., 1995), we did not observe such a linear increase of the blastoderm margin in goldfish embryos (Fig. 2).

To overcome this difficulty, we defined the "percentage of blastopore closure" as an additional index for the staging period; equivalent indices (for example, "yolk plug closure" and "area of blastoderm") were used in earlier studies of zebrafish, other teleost species, and amphibians (Kimmel et al., 1989; le Pabic et al., 2009; Latimer and Jessen, 2010; Kim et al., 2010). This index refers to the ratio between the maximum diameter of the blastopore and that of the blastoderm-covered yolk region along the DV axis (Fig. 9).

50%-epiboly

The thickness of the blastoderm begins to standardize at the 40–45%-epiboly stage (Fig. 8A) and is almost fully uniform by the 50%-epiboly stage (Fig. 8B). At this stage, most embryos have a slightly oval or roundish pear shape (Fig. 8B).

Germ ring

The percent-epiboly is almost the same as that at the 50%-epiboly stage. Under darkfield and oblique light, the germ ring can be observed as a stripe at the most vegetal pole-side of the blastoderm margin along the equatorial plane (Fig. 8C).

Shield

The embryonic shield can be observed as a prominence on the inner-side of the blastoderm margin, at the dorsal side of the embryo (Fig. 8D,E). From the 50%-epiboly stage to the shield stage, involution at the blastoderm margin seems to cause changes in the shape of the uncovered yolk.

60%-epiboly

More than half of the yolk is covered by the blastoderm (Fig. 8F). The percentage of blastopore closure is around 25–30%. The dorsal side of the blastoderm, including the embryonic shield, is obviously thicker than at the previous stage. The percentage of blastopore closure begins to increase (Figs. 8F–G, 9). As the shape of the yolk plug is highly variable during the late gastrula stage (from 60% to 90%-epiboly stages) (Kimmel et al., 1995), it is difficult to apply the percent epiboly index to these stages (Fig. 8G–M). This difficulty is one of the major reasons why we were unable to fit a reliable regression line to the hour post fertilization-stage plot (Fig. 2). However, the percentage of blastopore closure seems to be consistent with the other staging indices (for example, the rudiments of brain and polster) (Fig. 8F–M).

90%-epiboly

The tail bud prominence can be observed at the dorsal aspect of the blastopore after the 85%-epiboly stage (Fig. 8I–M). The yolk uncovered by the blastoderm takes the yolk plug shape, which can be observed in amphibian embryos (Keller et al., 1985; Kim et al., 2010). The neural plate is formed as a thick dorsal epiblast at the animal pole (Fig. 8I–L). Blastopore closure is around 70–80%.

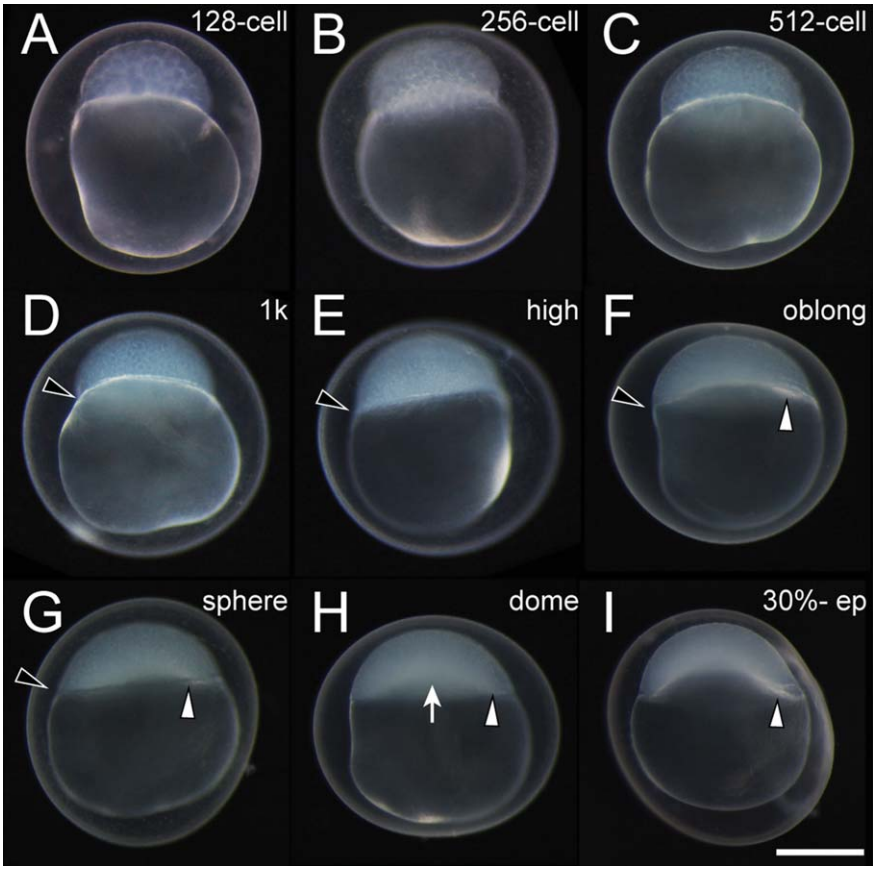

Fig. 6. **A–I**: Side views of goldfish embryos at the blastula stage. The black arrows indicate the boundary between the blastoderm and the yolk on the surface of 1k, high, oblong, and sphere stage embryos. White arrowheads and arrows indicate the internal margin between the blastoderm and the yolk in sphere, dome, and 30%-epiboly embryos. Scale bar = 0.5 mm.

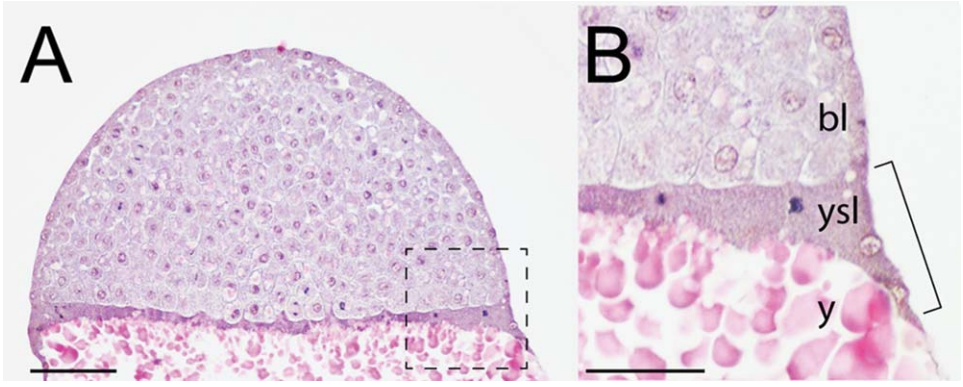

Fig. 7. Yolk syncytial layer of an early stage goldfish embryo. **A:** Histological section of a high embryo. **B:** Magnified view of the boxed area in A. The outer edge of the yolk syncytial layer is indicated by a bracket. bl, blastoderm; y, yolk; ysl, yolk syncytial layer. Scale bars = 100 μm in A, 10 μm in B.

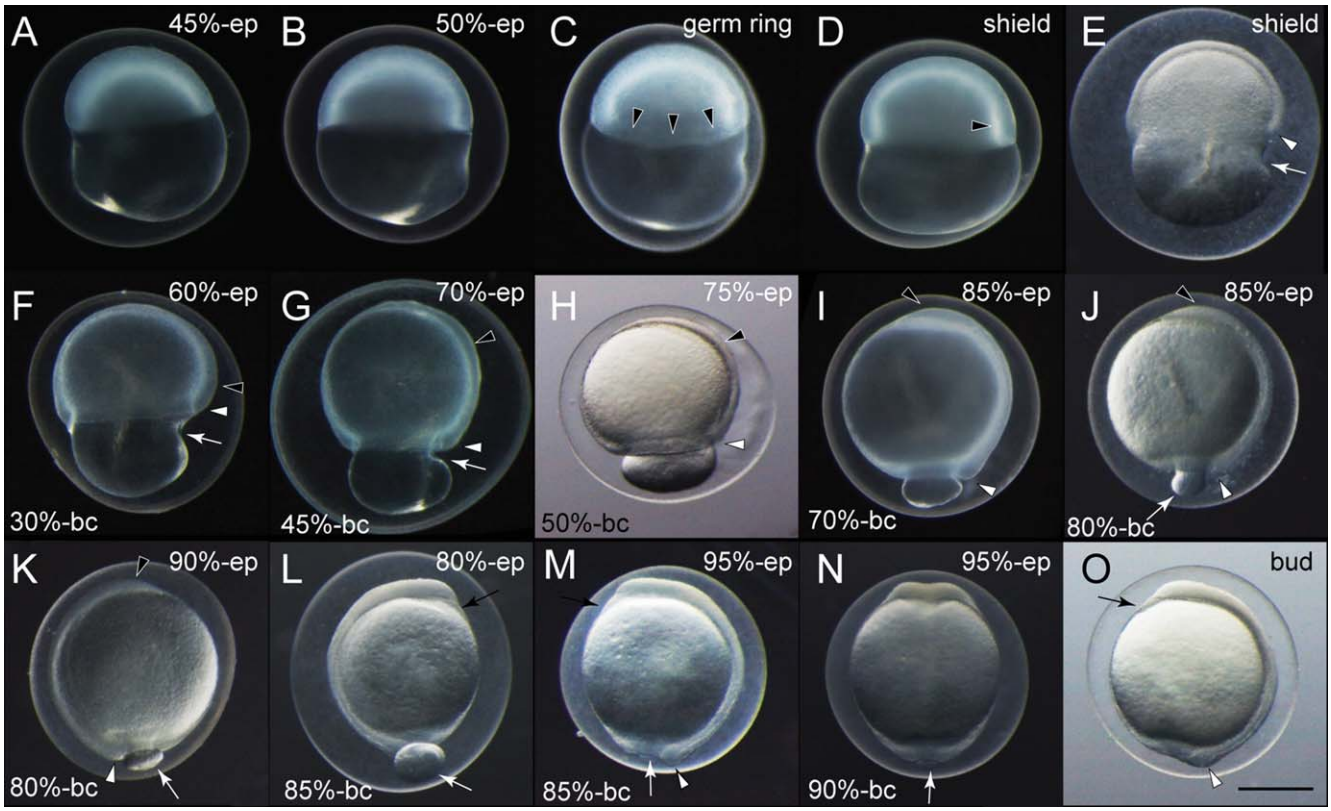

Fig. 8. Gastrula stages of goldfish embryos. **A:** Side view of a 45%-epiboly embryo. **B:** Side view of a 50%-epiboly embryo. **C:** Side view of a germ ring stage embryo. Black arrowheads indicate the germ ring. **D:** Left-side view of an early shield stage embryo. The thickness of the dorsal and ventral sides of the blastoderm are different at this stage (black arrowheads). **E:** Left-side view of a late shield stage embryo with oblique light. The embryonic shield is visible at the dorsal side of the blastoderm margin. The white arrowheads in E–K, M, and O indicate the dorsal side of the blastoderm margin. Most embryos from the late shield stage to the 70%-epiboly stage have a sharply curved surface at the yolk's dorsal side (indicated by the white arrows in E–G). **F:** Left-side view of a 60%-epiboly embryo. **G:** Left-side view of a 70%-epiboly embryo. The blastoderm at the anterior dorsal side is recognizably thicker after the 60%-epiboly stage (indicated by the black arrowheads in F–H). **H:** Left-side view of a 75%-epiboly embryo. **I:** Left-side view of an 85%-epiboly embryo showing 70% blastopore closure. The rudiments of the brain are indicated by black arrowheads in I–K. **J:** Left-side view of an 85%-epiboly embryo with oblique light, showing 80% blastopore closure. Yolk plugs in J–N are indicated by white arrows. **K:** Right-side view of a 90%-epiboly embryo. **L:** Right-side view of an 80% embryo. This embryo shows a well-developed polster and a large yolk plug (black and white arrows, respectively). **M:** Right-side view of a 95%-epiboly embryo. **N:** Ventral view of a 95%-epiboly embryo. **O:** Left-side view of a bud stage embryo. The numbers in the bottom-left hand corner of panels F–O indicate the percentage of blastopore closure (please see Fig. 8). ep, epiboly; bc, blastopore closure. Scale bar = 0.5 mm.

95%-epiboly

Early polster can be recognized in most embryos (Fig. 8M). Blastopore closure is around 85–90%. From the ventral view, the developing neural plate and exposing yolk can be observed (Fig. 8N).

Bud stage

The tail bud and polster are distinctly prominent (Fig. 8O). The blastopore is completely closed (100%-epiboly) in most embryos (Fig. 8O). One to five somites exist even before 100%-epiboly in a few embryos, as reported in the Atlantic cod (*Gadus morhua*) and Nile tilapia (*Oreochromis niloticus*) (Hall et al., 2004; Fujimura and Okada, 2007). In fact, a small amount of yolk is not covered by the blastoderm and is excluded from the embryo even during somite genesis (Fig. 10; also described in the next section).

Segmentation Period

Using somite number, we categorized the segmentation period of goldfish embryos into five stages (6-, 10-, 14-, 18-, and 22-somite stages, Fig. 9). As goldfish embryos at the late gastrula stage possess one to five somites, the gastrula stage and segmentation period overlap slightly (Fig. 2). In fact, somite development begins before the yolk is completely covered by the blastoderm, and the exposed yolk can be recognized at the 8- to 10-somite stage in a few embryos (Fig. 10A,B). With the exception of the exposed yolk, goldfish embryos share similar morphology and developmental processes with zebrafish embryos during the segmentation period (Kimmel et al., 1995). From the 6- to 25-somite stage, the rate of somite appearance is approximately two somites per hour in the goldfish (Fig. 2). This rate is largely consistent with that observed by Li et al. (1959).

6-Somite stage

Developing somites are cubical in shape. Horizontally elongated optic primordia are visible (Fig. 10A). The

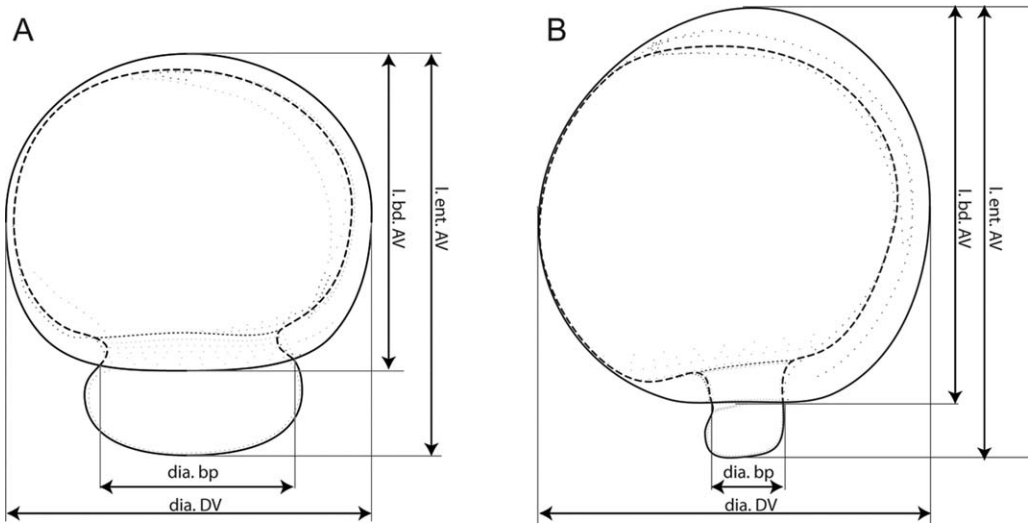

Fig. 9. Indices for staging of gastrula period embryos. **A,B:** Schematic drawing of early (A) and late (B) gastrula embryos. The percentage of epiboly and blastopore closure are defined as a percentage of l. bd.AV/l. ent.AV and dia.bp/dia. DV, respectively. dia.bp, diameter of blastopore; dia.DV, diameter of embryo along dorsal–ventral axis; l.bd.AV, length of blastoderm along the animal–vegetal pole axis. L.ent.AV. length of entire embryo along the animal–vegetal pole axis.

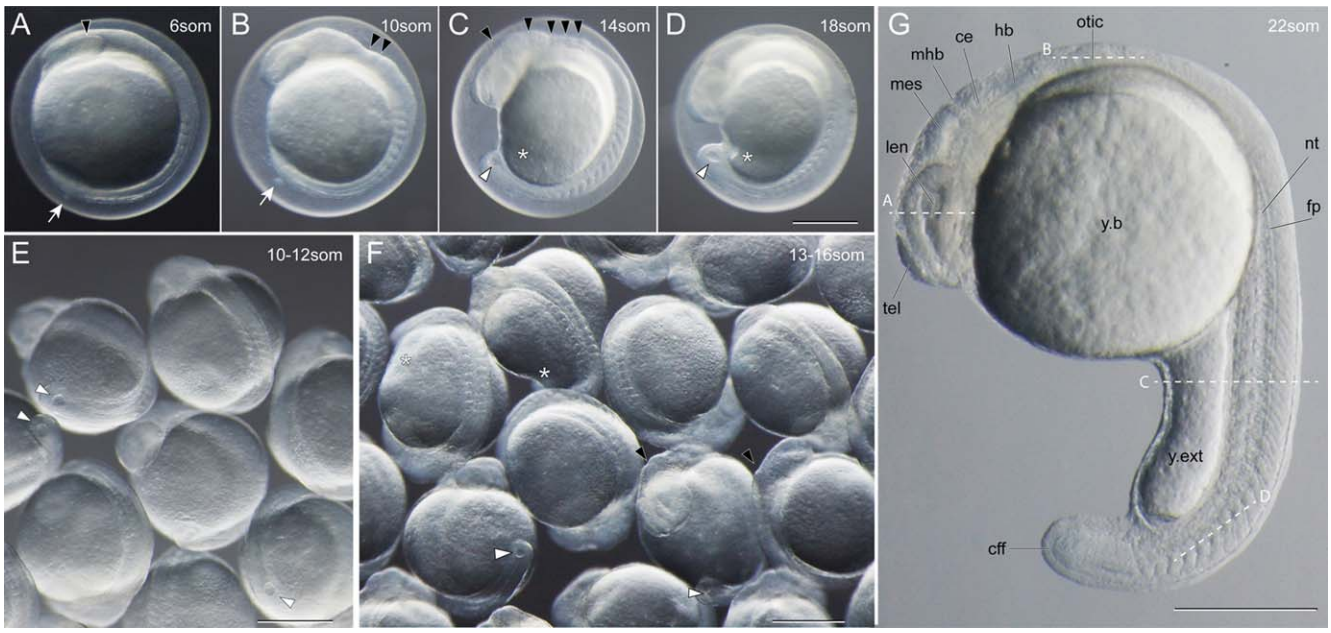

Fig. 10. Segmentation stage of goldfish embryos. **A:** Left lateral view of a six-somite stage embryo. The optic primordium is indicated by the black arrowhead. Exposed yolk is indicated by white arrows in A and B. **B:** Left lateral view of a 10-somite stage embryo. Divisions of the brain rudiment are indicated by black arrowheads. **C:** Left lateral view of a 14-somite stage embryo. The rudiment of cerebellum and rhombomeric regions are indicated by black arrowheads in C and F. Kupffer's vesicles are indicated by white arrowheads in C to F. **D:** Left lateral view of a 18-somite stage embryo. Construction of yolk is recognizable (white asterisk). **E:** Dechorionated 10–12 somite stage embryos. **F:** Dechorionated 13–16 somite stage embryos. **G:** Left lateral view of a 22-somite stage embryo. White hatched lines indicate approximate sectioned level in Figure 11. ce, cerebellum; cff, caudal fin fold; fp, floor plate; mes, mesencephalon; nt, notochord; otic, otic vesicle; tel, telencephalon; y. b, yolk ball; y. ext, yolk extension. Scale bar = 0.5 mm.

rudiment of the brain begins to subdivide.

10-Somite stage

The rudiment of the brain can be recognized as a prominence in the outline of the embryo head region (Fig. 10B). Subdivision of the telencephalon, diencephalon, mesencephalon, and rhombomeric region is evident. Anterior somites demonstrate a rounded rectangular shape. Kupffer's vesicles are readily visible in a posterior view of 10–12 somite embryos (Fig. 10E).

14-Somite stage

Somites have a V-shape (Fig. 10C). Subdivisions of the mesencephalon,

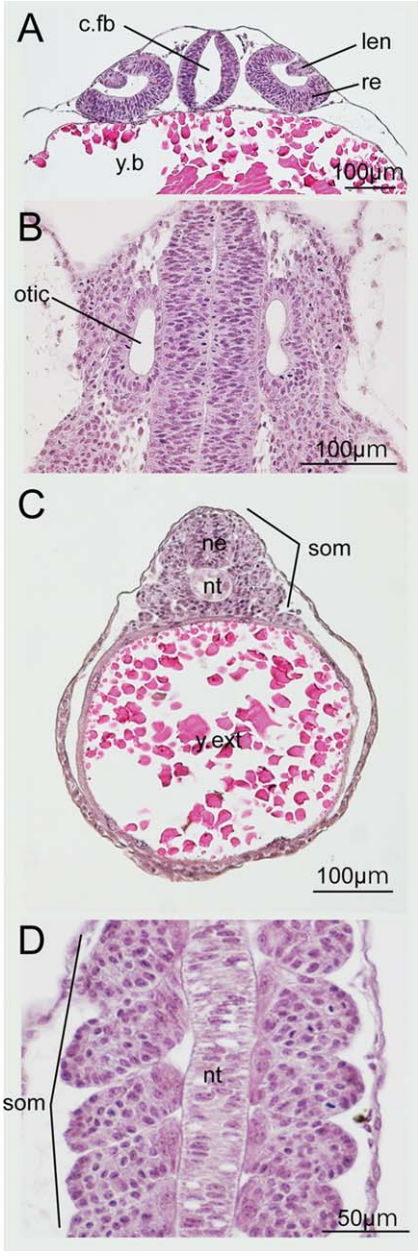

Fig. 11. Histological sections of 20- to 22-somite stage embryos. **A:** Transverse section at the optic level. **B:** Horizontal section at the otic level (the upside is posterior). **C:** Transverse section at the yolk extension level (220 μm anterior to the posterior end of the yolk extension). **D:** Horizontal section at the trunk level (the upside is anterior). c. fb, cavity of forebrain; len, lens; re, retinal primordia. Scale bars = 100 μm in A–C, 50 μm in D.

cerebellum, and rhombomeric region are visible, as also observed in 18-somite stage zebrafish embryos (Kimmel et al., 1995) (black arrowheads in Fig. 9C,F). The posterior part of yolk is slightly constructed and extended posteriorly, and begins to form a yolk extension (asterisks in Fig. 10C,F). Kupffer's vesicles can be seen in the lateral and posterior view of the protruded tail bud (white arrowhead in Fig. 9C,F).

18-Somite stage

The prominent tail bud is more evident than at earlier stages (Fig. 10C,D).

22-Somite stage

The brain primordia are highly sculptured. Lens primordia and otic vesicles are visible in live embryos (Fig. 10G) and in histological sections of embryos at approximately the equivalent stage (Fig. 11A,B). The floor plate is also visible at the dorsal aspect of the notochord (Fig. 10G). The rudiment of the median fin fold can be observed at the dorsal side of embryos at the somite levels. The yolk extension takes an elongated rod-like shape at approximately this stage (Fig. 10G). The median fin fold can be recognized at the posterior levels of the yolk extension (Abe et al., 2007). The yolk syncytial layer is visible at the yolk extension in histological sections (Fig. 11C). Twitching of the trunk muscles can be observed at this stage. Examinations of horizontal histological sections also reveal that the notochord is not vacuolated at this stage, and certain somite cells attached to the notochord are elongated in an anteroposterior direction (Fig. 11D).

Pharyngula Period

From the late segmentation stage (Fig. 10G), the yolk extension and post-cloacal region begin to elongate posteriorly, and this is followed by pigmentation and budding of the pectoral fin primordia (Fig. 12). The goldfish embryos in this period were staged using the pigmentation patterns in the retina and embryo surface, and the fin budding patterns described by Kajishima (1960). Conversely, zebrafish embryos in this period were designated based on the degree of extension of the lateral line primordium (prim stages) (Kimmel et al., 1995).

The prim staging index is one of the best objective staging indices for thin and highly transparent teleost fish embryos. However, with the exception of the zebrafish staging system (Kimmel et al., 1995), no reported teleost system uses the prim index (Swarup, 1958; Armstrong and Child, 1965; Benzie, 1968; Ballard, 1973; Kimmel et al., 1995; Martinez and Bolker, 2003; Iwamatsu, 2004; Hall et al., 2004; Fujimoto et al., 2004; Fujimura and Okada, 2007; Hinaux et al., 2011). This staging system seems to be suitable for the eggs of flounder, tilapia, and cavefish (Martinez and Bolker, 2003; Fujimura and Okada, 2007; Hinaux et al., 2007), but descriptions of the lateral line primordium are not found in reports of these organisms. This may be due to the difficulty and effort required for optimizing observations of the lateral line primordia, as indicated in Kimmel et al. (1995). We were also unable to apply this staging index and these observation methods to goldfish embryos directly, because of their reduced transparency, whitish color, thicker body, and relatively large yolk; these properties impeded optimization of the conditions for differential interference contrast (DIC) microscopic observation of the lateral line primordia.

In lieu of DIC microscopy, we used a stereomicroscope with oblique light to observe lateral line primordia (see the Experimental Procedures section). We were able to trace lateral line primordia in late pharyngula stage goldfish embryos embedded on agar plates; the lateral embryonic sides of these embryos could be observed with the same depth of focus. However, we could not identify lateral line primordia in early pharyngula stage embryos, because at this stage, the anterior half of the embryonic part is curved, thick, and less transparent (Fig. 12). Thus, for stage identification during this period, we examined "otic vesicle closure" (OVC) (Fig. 13). This index corresponds with "otic vesicle length" (OVL) (Kimmel et al., 1995). OVC increases from approximately 20% at the beginning of the pharyngula period to over 60% at the end, being inversely proportional to OVL.

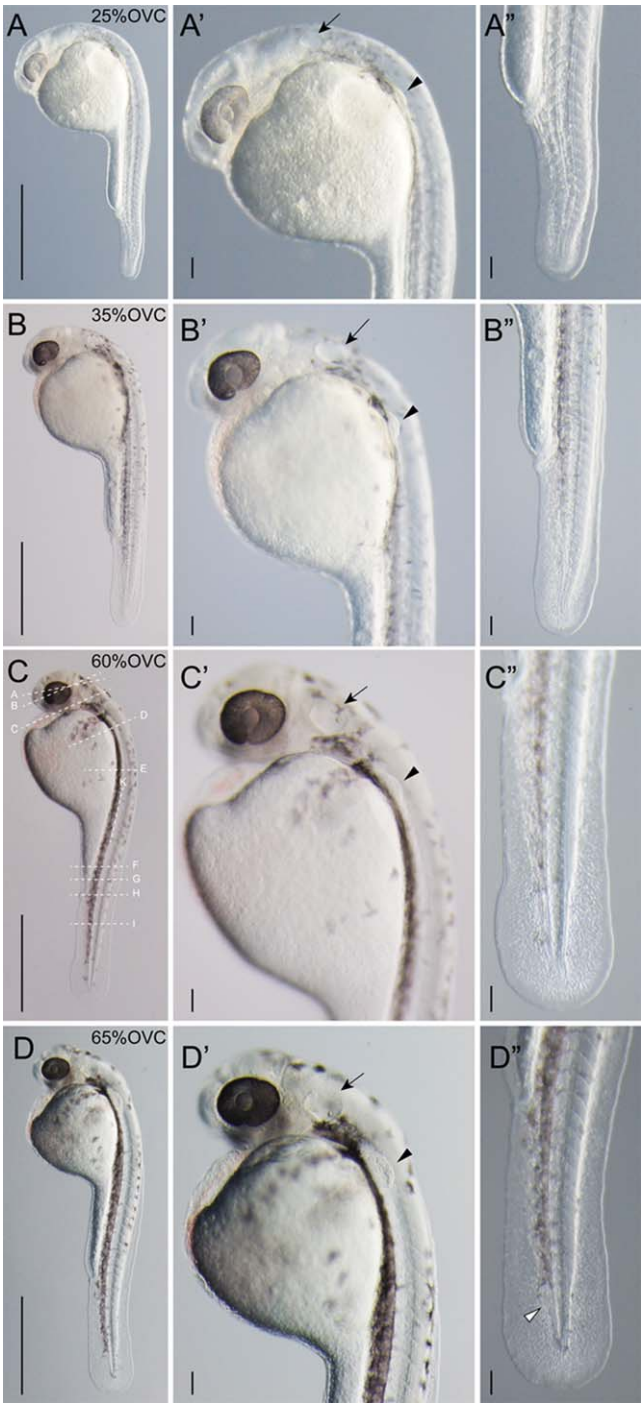

Fig. 12. Pharyngula stage of goldfish embryos. **A:** 25% OVC-somite stage embryo. **B:** 35% OVC stage embryo. **C:** 60% OVC stage embryo. White hatched lines indicate the approximate sectioned levels in Figure 14. **D:** 65% OVC stage embryo. **A′–D″:** Panels in the center and right-hand columns show magnified views of the anterior and posterior regions in the same embryos, respectively. Pectoral fin buds and otic vesicles are indicated by black arrowheads and arrows, respectively. The white arrowhead indicates a gap in the melanocyte pattern at the caudal level in the ventral aspect. OVC is defined in Figure 13. Scale bar = 1 mm in A–D, 0.1 mm in A′–D″.

Based on OVC, we categorized goldfish embryos in the pharyngeal period into three different stages (25% OVC, 35% OVC, and 65% OVC; Table 2; Fig. 13). We also examined histological sections of 60% OVC embryos, to inspect the development of tissues and organs (Fig. 14).

25% OVC

Retina and skin show early pigmentation (Fig. 12A). Otic vesicles form an ellipse (black arrow in Fig. 12A′). Blood flow in the common cardinal vein (duct of Cuvier) (Reib, 1973; Zhong, 2005) and a heartbeat are present. The pectoral fin buds appear (black arrowhead in Fig. 12A′). The curved yolk extension and caudal region straighten by the late segmentation stage (Figs. 10G, 12A). More than 30 somites are visible in total. At the post-cloacal level, 14 somites can be observed (Fig. 12A,A″). Median fin folds appear at the dorsal and ventral side of the caudal area (Fig. 12A″), as in zebrafish (Abe et al., 2007). From this stage, the embryo length (EL) evidently changed. At this stage, EL = 2.8 mm. Based on these characteristics, this stage in goldfish seems to be equivalent with the Prim-5 stage in the zebrafish staging table (Fig. 12A–A″) (Kimmel et al., 1995).

35% OVC

The appearance of goldfish embryos at this stage is also similar to that of zebrafish embryos of the prim-10 to −20 stages (Fig. 12B–C″) (Kimmel et al., 1995). In several individuals, lateral line primordial can be recognized at the yolk extension level. The retina is strongly pigmented at this stage (Fig. 12B,B′). A strong heartbeat can be observed. The pectoral fin bud is more prominent by this stage (arrowhead in Fig. 12B′,C′) and melanocyte distribution is broader (compare Fig. 12B–B″ with Fig. 12C–C″). The caudal part of the median fin fold dramatically changes in size during this stage; the caudal fin fold of 60% OVC embryos (Fig. 12C″) is broader than that of 35% OVC embryos (Fig. 12B″). The otic vesicle also changes from an ellipse to a round shape (black arrows in Fig. 10B′,C′).

Histological examination of later stages (equivalent to 60% OVC; Fig. 14) confirmed the presence of the telencephalon, developing nasal pit, liver, and heart ventricle and atrium (Fig. 14A–D) (Stainier and Fishman, 1992; Field et al., 2003). The yolk syncytial layer (from the mid trunk region to the end of the yolk extension) can be readily distinguished

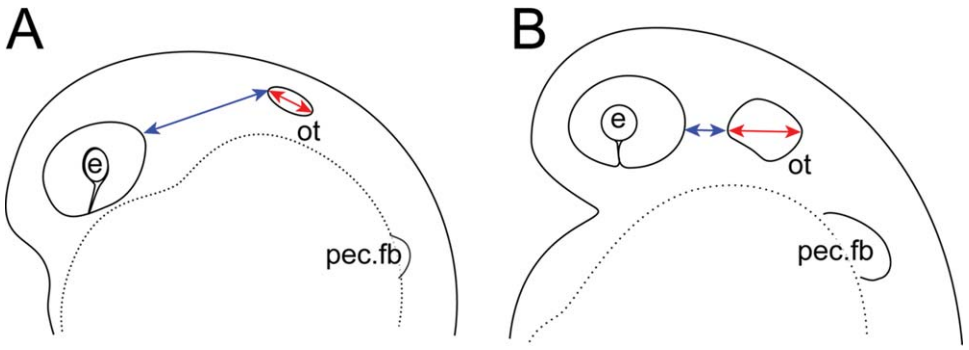

Fig. 13. Indices for staging of embryos during the pharyngula period. **A,B:** Schematic drawings of early (A) and late (B) pharyngula embryos. Blue arrows indicate the shortest distance between the posterior end of the eye and the anterior end of the otic vesicle (dist. e. ot). Red arrows indicate the length of the major axis of the otic vesicle (l. ot). The percentage of otic vesicle closure (OVC) is defined as l. ot/l. ot + dist. e. ot. e, eye; ot, otic vesicle; pec. fb, pectoral fin bud.

from the other tissues (Fig. 14E–G). In addition, the yolk syncytial layer is noticeably thicker at the posterior end of the yolk extension than elsewhere (Fig. 14G). Pronephric ducts can be observed at the lateral aspect of the intestinal tract, from the mid trunk to the cloacal level (Fig. 14E–H) (Ng et al., 2005). Median fin folds consist primarily of ectodermal epithelial cells, but also contain some mesenchymal cells (Fig. 14G–I). Myotomes are located at the lateral aspect of the neural tube, notochord, and dorsal aorta (Fig. 14D–I). Horizontal myoseptum can be identified in several transverse sections (Fig. 14F–H), and anteroposteriorly elongated myotomes can be observed in horizontal sections of the trunk region (Fig. 14J). In a single myotome, several multinucleated muscle fibers can be observed (Fig. 14J). Furthermore, the notochord is vacuolated by this stage (Fig. 14C–J). Several mesenchymal cells are distributed at the lateral aspect of the notochord at the head level (Fig. 14C). At this stage, the EL is around 3.4–3.5.

65% OVL

At this stage, the lateral line primordia extend to the trunk region at the 20th to 26th somite (or myosepta) level. There is greater contrast between pigmented and nonpigmented areas (Fig. 12D–D″). The melanocyte on the yolk ball tends to distribute around the common caudal vein, and pigmented regions extend from ventral to lateral (Fig. 12D′). A gap in the melanocyte pattern at the caudal level in the ventral aspect is clearly recognizable in most of the embryos (white arrowhead in Fig. 12D″) (Parichy et al., 2009). The pectoral fin bud takes an anteroposteriorly asymmetric shape; the height to width ratio of the pectoral fin bud is greater than 0.5 (black arrowhead in Fig. 12D′). The anterior face of the pectoral fin bud slopes relatively smoothly (Fig. 12D′). At this stage, EL = 3.6.

Hatching Period

Hatching time cannot be used as an index for staging in goldfish, because it differs greatly between individuals, and is also affected by several environmental factors (for example, temperature, egg density, oxygen concentration, and others) (Kimmel et al., 1995; Yamaha et al., 1999). Goldfish tend to hatch out at around 3 days post fertilization (60 to 72 hpf) at 25°C (Li et al., 1959; Fig. 3), but their hatching time and stages are not always synchronized among individuals, even for the same batch of embryos (Yamaha et al., 1999).

The goldfish staging system described by Li et al. (1959) follows development of the vein and median fins. On the other hand, staging of zebrafish embryos and larvae involves pigmentation patterns (distribution of melanophores, xanthophores, and iridophores), the shape of the pectoral fin bud, and the head–trunk angle (HTA) (Kimmel et al., 1995). After 48 hpf at 24°C, goldfish embryos and larvae also show xanthophore pigmentation patterns and evident elongation of the fin bud and fins (Figs. 15, 16), which cannot be observed in the pharyngula period (Fig. 12). By applying the above characteristics and following the zebrafish nomenclature systems (Kimmel et al., 1995), we categorized goldfish embryos and larvae in this period into three stages: long pec, pec-fin, and protruding mouth (Figs. 15–17). We also conducted histological analysis of late-stage larvae in this period (Fig. 18).

Long pec

The dorsal side of the larvae, from the head to anterior half trunk regions, are pale yellow (xanthophores) (Fig. 15A). Melanophores were increased on the dorsal side of the head and the common cardinal vein. The common cardinal vein can be recognized as a black tube in the lateral view (Fig. 15A′). From this stage, the pectoral fin bud is elongated posteriorly, extending the height-to-width ratio to approximately 1.5 (Fig. 16A). The caudal part of the median fin fold is enlarged, and begins to expand in a dorsoventral direction (Fig. 15A). The HTA is approximately 40°, although there is variation between individuals. The angle in goldfish embryos at this stage is narrower than that of the zebrafish equivalent (Kimmel et al., 1995). Several embryos at this stage have already opened their mouth on the ventral aspect of the head (Fig. 15A).

Pec fin

The xanthophore colored area extends to the caudal level (Fig. 15B), and the melanophore-pigmented region of the common cardinal vein extends

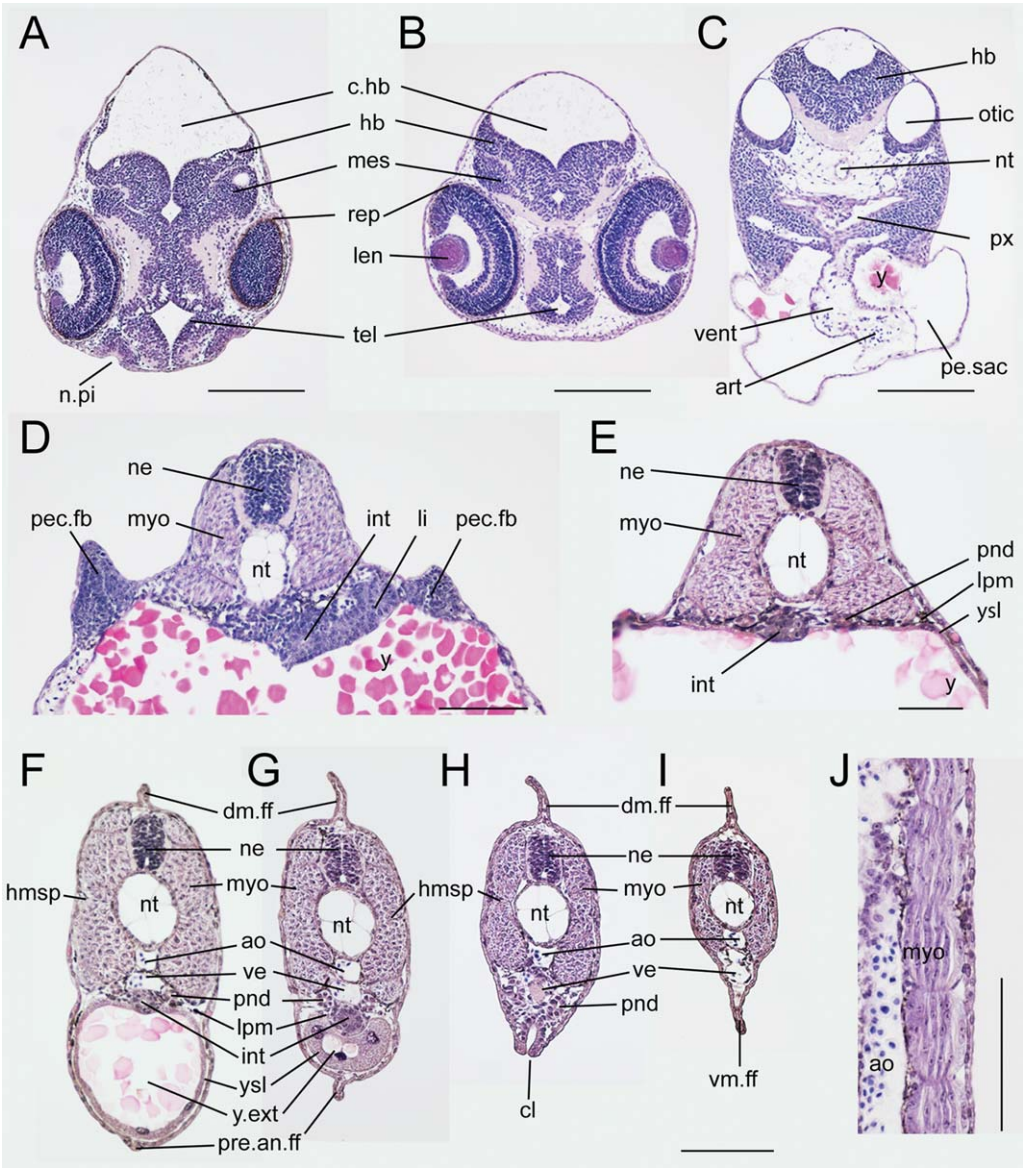

Fig. 14. Histological sections of embryos during the pharyngula period. **A:** Horizontal section at the nasal pit level. **B,C:** Transverse sections at the optic (B) and otic (C) levels, respectively. **D:** Transverse section at the level of the pectoral fin bud. **E–I:** Transverse sections at the level of the anterior yolk extension (approximately 400 μm anterior to the posterior end of the yolk extension; E), the posterior yolk extension (approximately 100 μm anterior to the posterior end of the yolk extension; F), the posterior end of the yolk extension (G), cloaca (H), and post cloacal region (approximately 300 μm posterior to the cloaca; I). **J:** Horizontal section of the trunk region. All of the sections are derived from approximately 60% OVC stage embryos. Two sets of sections (B–D and E–I) are derived from identical individuals. ao, dorsal aorta; art, atrium; c.hb, cavity of hindbrain; cl, cloaca; dm.ff, dorsal median fin fold; hb, hindbrain; hmsp, horizontal myoseptum; otic, otic vesicle; int, intestinal tract; len, lens; li, liver; lpm, lateral plate mesoderm; mes, mesencephalon; myo, myotome; n.pi, nasal pit; ne, neural tube; nt, notochord; pe.sac, pericardial sac; pec.fb, pectoral fin bud; pnd, pronephric duct; pre.an.ff, pre-anal fin fold; px, pharynx; rpe, retinal pigment epithelium; tel, telencephalon; vm.ff, ventral median fin fold; ve, axial vein; vent, ventricle; y, yolk; ysl, yolk syncytial layer. Scale bars = 100 μm.

ventrally (Fig. 15B′). The head of this stage tilts upward slightly more than that at the long pec fin stage; the HTA is approximately 30°. The pectoral fin bud forms a blade-like shape, and has actinotrichia which will develop into the fin ray (Fig. 16B–D). At this stage, an approximate two-fold increase in the size of the apical fold of the pectoral fin was observed, as for zebrafish (Fig. 16C,D) (Yano and Tamura, 2013). In addition, the mouth opens anteroventrally (Fig. 17B). In the eyes at this stage, six different layers (ganglion cell layer, inner plexiform layer, inner nuclear layer, outer plexiform layer, outer nuclear layer, retinal pigment epithelium) can be observed, as in zebrafish (Fig. 18A) (Gross et al., 2005). At the cranial level, chondrogenesis of parachordal and trabecula cartilage can be observed; at the otic vesicle level, mesenchymal cells at the lateral aspects of the notochord secrete Alcian blue-positive extracellular matrix (Fig. 18B) (Schilling and Kimmel, 1997).

Protruding mouth

The dorsal side of the larvae is pigmented by xanthophores (Fig. 15C). The outline of the dorsal side of the

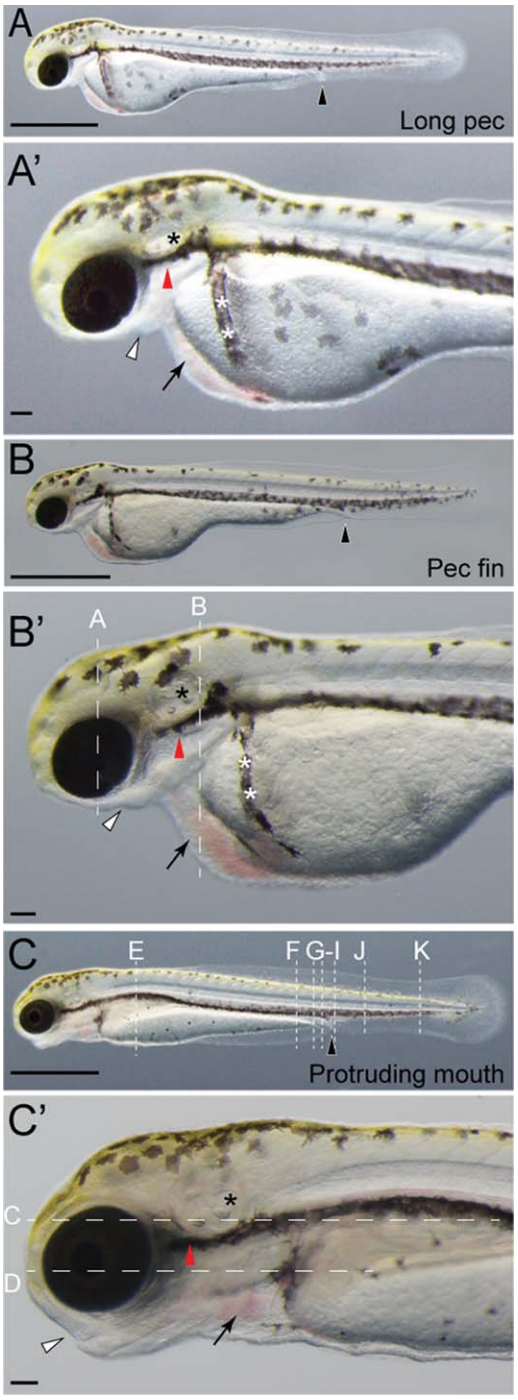

Fig. 15. Hatching stage of goldfish larvae. **A:** Long pec stage embryo. A′: Magnified view of the anterior part of the long pec stage embryo in A. **B:** Pec stage embryo. **B′:** Magnified view of the anterior part of the pec stage embryo in B. **C:** Protruding mouth stage embryo. **C′:** Magnified view of the protruding mouth stage embryo in C. Anatomical features are indicated as follows: White arrowheads: mouth; black arrowheads: cloacae; black arrows: heart; black asterisks: otic vesicles; white asterisks: common cardinal vein; and red arrowheads: anterior horn. Scale bars = 1 mm in A,C,E, 0.1 mm in B,D,F.

head is almost straight; the HTA is approximately 20°. The position of the heart is evidently different between the former two stages and this stage; the heart moves to the anterior, and is located at the anterior aspect of the yolk at this stage (black arrows in Fig. 15A′,B′,C′). Under oblique transparent light, a cartilaginous structure can be observed in the ventral cranial region in the live larvae (Fig. 15C′). Horizontal sections of the anterior part of the larvae reveal cartilaginous tissues at the anterior aspect of the otic vesicles, the lateral side of the notochord, the pectoral fins, and the hyoid and branchial arches (Fig. 18C,D) (Kimmel et al., 1995; Schilling and Kimmel, 1997). Mouth openings at this stage are more anterior than at the pec fin stage (Fig. 15B′,C′). The developing swim bladder was observed in transverse sections at the level of the posterior end of the pectoral fin (Fig. 18C) (Ng et al., 2005). The outline of the ventral median fin fold is not continuous; a gap at the cloacal level divides the pre- and post-cloacal fin folds (black arrowhead in Fig. 15C). This gap is not observed at the long-pec or pec fin stage (black arrowheads in Fig. 15A,B). The caudal median fin fold is larger than at earlier stages (Fig. 15C). Alcian blue-positive tissues are observed in all median fin folds (Fig. 18F–K). Well-developed muscle tissues and vertical myosepta are present in horizontal sections at the trunk level (Fig. 18L). Almost all embryos have hatched by this stage.

DISCUSSION

In contrast to previous studies that used unspecified goldfish strains (Li et al., 1959; Kajishima, 1960; Otani et al., 2002), we have described the embryonic and larval morphology of the common goldfish strain, which exhibits wild-type goldfish morphology (slender body and short fins) (Figs. 1A, 4–6, 8, 10, 12, 15). In addition, we have described the histology of embryonic and larval tissues at several stages (Figs. 7–18). Our present staging table is the first normal development table of the wild-type goldfish, covering the zygote to hatching stages (Table 2). These results suggest that the embryonic morphology of goldfish and zebrafish are, in general, comparable (Kimmel et al., 1995). However, we also identified several different embryonic features between these two teleost species.

One of the most significant differences between zebrafish and goldfish is the texture of the yolk. The yolk of goldfish embryos is softer and larger than that of zebrafish embryos

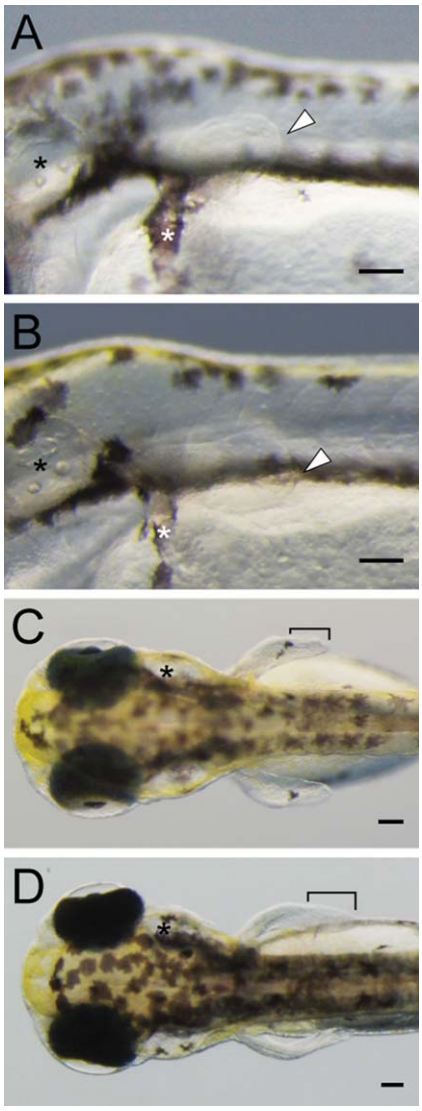

Fig. 16. Pectoral fin of hatching stage larvae. **A:** Left lateral view of the pectoral fin in long pec fin stage larva. **B:** Left lateral view of the pectoral fin in pec fin stage larva. **C:** Dorsal view of early pec fin stage larva. **D:** Dorsal view of late pec fin stage larva. A,B: The distal end of the pectoral fin is indicated by white arrowheads in A and B. C,D: The width of the yolk along the lateral axis is narrower in early pec fin larva (C) than in late pec fin larva (D); brackets indicate the apical fold of the pectoral fin. Otic vesicles and pigmented common cardinal veins are indicated by black and white asterisks, respectively. Scale bars = 0.1 mm

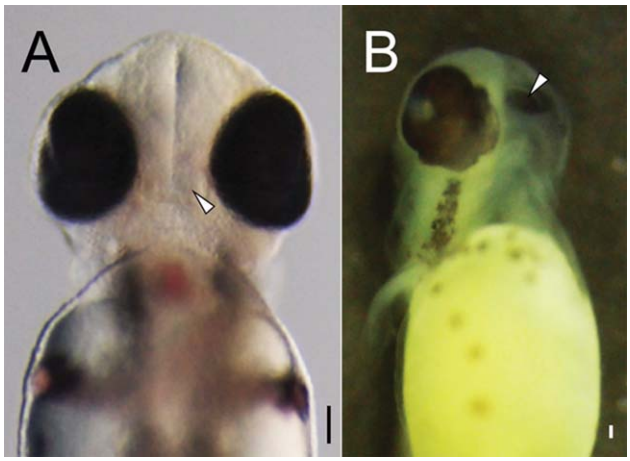

Fig. 17. Mouth opening of hatching stage larvae. **A:** Ventral view of the head of a long pec fin stage embryo. **B:** Oblique ventral view of the head of a pec fin stage embryo. Pec fin stage embryos were fixed with Bouin's fixative. White arrowheads indicate mouth opening. Scale bars = 0.1 mm.

(Figs. 4–6, 8, 10). This goldfish-specific yolk texture caused difficulties in stage identification during the late blastula stage in previous studies (Yamaha et al., 1999; Otani et al., 2002); despite these challenges, we succeeded in categorizing goldfish late blastula stages embryos into high, oblong, sphere, and dome stages (Fig. 8). Inconsistencies between our study and previous studies seem to be related to whether the descriptions were based on dechorionated embryos or not; previous studies primarily used dechorionated embryos (Yamaha et al., 1993, 1998, 1999; Mizuno et al., 1997, 1999; Otani et al., 2002), while we used nondechorionated blastula, gastrula, and early segmentation stage embryos for the embryonic descriptions (Figs. 6–10). Given that yolk shape can be easily changed by its own weight, it is conceivable that stage identification is more difficult using dechorionated goldfish embryos at the late blastula stages.

The most significant specific feature of goldfish yolk is the way its texture and size varies between individual embryos (Fig. 8G–N) (Yamaha et al., 1999). In fact, we were able to identify variations in the epiboly process between individual goldfish embryos (Fig. 8G–N), which were reflected as exposed yolk at the posterior aspect of the tail bud in early segmentation stage embryos (Fig. 10A,B). Thus, although the development of segmentation stage goldfish embryos is similar to that of zebrafish (Fig. 10), it is feasible that variations in the yolk size affect other embryonic features. For example, the relative position of the Kupffer's vesicles may differ between large yolk and small yolk goldfish embryos, on the basis of posterior body development in zebrafish (Kanki and Ho, 1997). Moreover, while it is still unclear how variations in yolk size affect the formation of the yolk syncytial layer, our histological observations suggest that the yolk syncytial layer pattern in high-stage embryos is similar between zebrafish and goldfish (Fig. 7) (Kimmel et al., 1995; Carvalho and Heisenberg, 2010). Further investigation will be required to confirm whether variations in yolk size affect subsequent embryonic morphology, and developmental rate.

From the pharyngula to hatching periods, the following three characteristics are clearly different between goldfish and zebrafish: hatching gland, melanocyte pigmentation patterns, and mouth opening (Figs. 12, 15). We were unable to identify the distributing location of the hatching gland through observations of live goldfish using stereomicroscopy (Fig. 12). This seems to be due to the broad and indistinct distribution patterns of the hatching gland in goldfish embryos (Ouji, 1955; Ishida, 1985). Examination of melanocyte distribution patterns revealed differences in the "dorsal stripe," "ventral stripe," and "anterior horn" in goldfish and zebrafish (Fig. 15) (these terms are defined in Kimmel et al., 1995). Melanophores begin to cluster, and the dorsal stripe subsequently appears at the dorsal aspect of pharyngula stage embryos in zebrafish (Kimmel et al., 1995), while such a distinctive

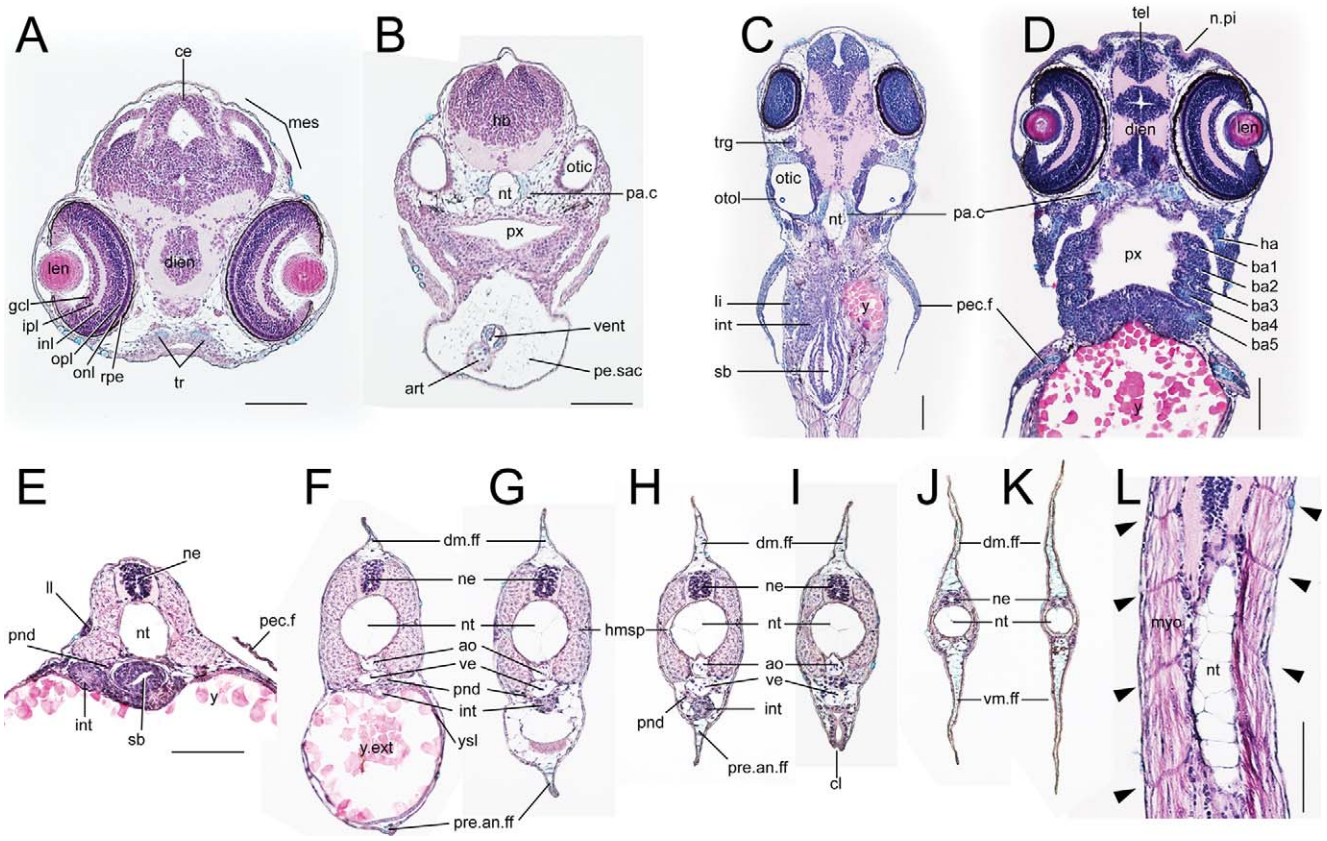

Fig. 18. Histological sections of hatching stage larva. **A,B:** Transverse sections at the eye and otic levels, respectively. **C,D:** Horizontal sections at the otic vesicle and eye levels, respectively. **E–K:** Transverse sections at the levels of the posterior end of the pectoral fin (E), the yolk extension (approximately 260 μm anterior to the posterior end of the yolk extension; F), the posterior end of the yolk extension (G), the pre-anal region (100 μm posterior to the posterior end of the yolk extension; H), cloaca (I), and post cloacal regions (330 and 1,000 μm posterior to cloaca; J and K). **L:** Horizontal section of trunk. Arrows indicate myoseptum. Two sets of sections (A,B and C–K) are derived from identical individuals. Sections were stained with eosin, haematoxylin, and Alcian blue. ao, dorsal aorta; art, atrium; ba, branchial arch; ce, cerebellum; cl, cloaca; dien, diencephalon; dm.ff, dorsal median fin fold; gcl, ganglion cell layer; ha, hyoid arch; inl, inner nuclear layer; int, intestinal tract; ipl, inner plexiform layer; li, liver; mes, mesencephalon; myo, myotome; n.pi, nasal pit; ne, neural tube; nt, notochord; onl outer nuclear layer; opl, outer plexiform layer; pa.c, parachordal cartilage; pe.sac, pericardial sac; pec.f, pectoral fin; pnd, pronephric duct; pre.an.ff, pre-anal fin fold; rpe, retinal pigment epithelium; sb, swim bladder; tel, telencephalon; tr, trabecula; trg, trigeminal ganglia; ve, axial vein; vent, ventricle; vm.ff, ventral median fin; y, yolk; y.ext, yolk extension; ysl, yolk syncytial layer. Scale bars = 100 μm. E–K are shown at the same magnification.

melanophore stripe was not observed in goldfish embryos (Fig. 15). On the other hand, the ventral stripe at the caudal level became visible earlier in goldfish than in zebrafish (Fig. 12A″,B″,C″,D″). In late pharyngula goldfish embryos, melanophores distribute at the ventral aspect of the notochord at the caudal level, forming a stripe associated with the dorsal aorta and vein (Fig. 12C″,D″); this is not observed in their zebrafish equivalents (Kimmel et al., 1995). In addition, the timing of anterior horn appearance seems to be slightly later in goldfish than in zebrafish embryos (Fig. 15). In zebrafish embryos, the anterior horn can be recognized as an extension of the ventral stripe at the dorsal aspect of the yolk, and this melanocyte stripe emerges at the levels of the eyes in prim-25 stage zebrafish embryos. However, the goldfish anterior horn begins to form at the equivalent stage (late pharyngula stage; 65% OVC), and finally appears at the early hatching stage after the appearance of the xanthophore (Figs. 12D,D″,15A,A′). Although there is variation between individuals, most of the populations exhibit the above tendencies.

In contrast to the development of pigmentation patterns, the timing of mouth opening is earlier in goldfish than in zebrafish (Fig. 17). A small open mouth was observed in pec-fin stage zebrafish embryos (Kimmel et al., 1995), while goldfish larvae at the equivalent stage exhibit a significantly larger opened mouth (Fig. 17B). These cranial embryonic morphological differences seem to reflect the adult morphology and feeding behavior. Although no significant difference was detected in the larval cranial structure in our study, these above-mentioned embryonic and larval morphologies should be carefully compared between goldfish and zebrafish (Schilling and Kimmel, 1997).

We suggest it is also worth considering the similarities (or otherwise) between the embryonic development of wild-type and mutant goldfish strains. Of the three previous reports of goldfish developmental stages (Li et al., 1959; Kajishima, 1960; Yamaha et al., 1999), only Kajishima (1960) mentioned differences in embryonic morphology between the common goldfish and mutant strains. This

earlier study provided sketches of pharyngeal stage embryos and larvae with bifurcated fin folds, and the descriptions are consistent with two previous reports which described prehatching embryonic and larval morphology of goldfish mutants (Watase, 1887; Hervey and Hems, 1948). It seems to be possible to distinguish the wild-type from the mutant at these stages, because of their morphological similarities with the adult.

However, Kajishima (1960) did not compare early-stage embryo morphology between the wild-type and mutant strains. Although illustrations of several early-stage embryos were provided, their strain was not identified (as mentioned in the Introduction section). Therefore, we were unable to determine whether these illustrations represent wild-type or mutant embryos, necessitating further embryonic comparison of wild-type and mutant strains (Fig. 1A,B).

As well as developmental background, differences in genetic background between goldfish and zebrafish should be noted. Classic cytogenetic, molecular evolutionary, and genomic studies have indicated that recent genome duplications occurred in the carp and goldfish lineages after these species diverged from zebrafish (Ohno et al., 1968; Ojima, 1983; Risinger and Larhammar, 1993; Larhammar and Risinger, 1994; Yang and Gui, 2004; Luo et al., 2006). This suggests that goldfish have an additional set of paralogous genes in their genome. Recently, the gene responsible for the mirror carp (a scaleless mutant carp), which is also derived from artificial selection, was identified through a zebrafish mutagenesis strategy (Rohner et al., 2009). This success with mirror carp has prompted others to compare previously isolated zebrafish mutants with various goldfish strains with divergent morphologies (Koh, 1931, 1932; Mullins et al., 1994, 1996; Neuhauss et al., 1996; vanEeden et al., 1996a,b; Hammerschmidt et al., 1996; Asano and Kubo, 1972; Smartt, 2001; Amsterdam et al., 2004; Komiyama et al., 2009).

Although the duplicated nature of the goldfish genome has previously hindered its genetic analysis, it is anticipated that the development of next generation sequencing techniques will overcome this hurdle (Metzker, 2010; Davey et al., 2011); while there are currently 10,969 expressed sequence tags (ESTs) available for goldfish, this number is expected to increase in the near future. Thus, goldfish may become an attractive model organism in which to investigate the relationships between genome duplication, developmental mechanisms, and morphological evolution (Holland and Garcia-Fernàndez, 1996; Amores et al., 1998; Hoegg et al., 2004; Jaillon et al., 2004; Meyer and Van de Peer, 2005; Sèmon and Wolfe, 2007; Sato and Nishida, 2010).

Comparative studies of goldfish and other teleost species may increase our understanding of genome duplication, as well as other evolutionary processes. For example, comparison of the morphology of goldfish and spontaneous mutants of medaka may determine whether or not similar mutant phenotypes arose from independent mutations of the same developmental mechanisms in different lineages. Such comparisons may be facilitated by the large number of spontaneous medaka mutant strains available (Takeda and Shimada, 2010). Furthermore, it may be possible to contrast the effects of artificial and natural selection by comparing goldfish strains to teleost species with highly divergent morphology arising from natural selection (such as stickleback, cichlid, and cavefish; Yamamoto and Jeffery, 2000; Peichel et al., 2001; Jeffery, 2001; Colosimo et al., 2004, 2005; Yamamoto et al., 2004, 2009; Kimmel et al., 2005; Albertson et al., 2005; Cresko et al., 2007; Kitano et al., 2008; Chan et al., 2010; Shapiro et al., 2004). We hope that our developmental stages will facilitate studies into the molecular developmental biology of goldfish, thereby providing insights into the evolutionary relationship between selection and developmental mechanisms.

EXPERIMENTAL PROCEDURES

Fish Samples

Adult individuals of the common goldfish strain (the single tail "*Wakin*") were purchased from the aquarium fish agency in Taiwan on March 2011. This strain is Japanese in origin. To avoid confusion derived from differences in goldfish nomenclature systems used by breeders and researchers (Matsui, 1934; Smartt, 2001), goldfish individuals with a slender body and a short single fin are referred to as the common goldfish (Fig. 1) in accordance with Smartt (2001); this definition includes *Funa-wo Wakin* and the single fin *Wakin*, as defined by Matsui (1934) and Matsui and Axelrod (1991). In total, 50 male and 50 female goldfish were separated and maintained in different cages in the same aquarium tanks (4000 liters in water volume). The aquarium tanks were kept under natural temperature conditions (14–24°C).

Artificial Fertilization

On April 2011, sperm were taken from several males and preserved in Modified Kurokura's extender 2 solution (Magyary et al., 1996) at 4°C, and eggs were squeezed out from mature females into Teflon coating dishes. Artificial fertilization was performed using dry methods. The fertilized eggs were spread onto 9-cm Petri dishes and 3-L aquarium tanks, containing tap water (22–24°C), as appropriate. Serial ID numbers were provided for male and female individuals used for artificial fertilization. One or two 9-cm Petri dishes containing 50–100 individuals were incubated until hatching, and the morphology and survival rate of the hatched larvae were recorded.

Microscopic Observation and Photography

For the observation of early stage embryos, fertilized eggs were spread onto 9-cm Petri dishes at a low density (less than 200 eggs/Petri dish). Eggs attached tightly to the surface of the Petri dish were surveyed. The position of each egg was marked to enable repeated monitoring of the same embryo. For the observation of late embryos, the egg chorion was removed by fine forceps or enzyme treatment modification zebrafish protocols, as appropriate (Westerfield, 2000). The dechorionated embryos

and hatched larvae were anesthetized using MS222 (tricaine methanesulfonate). The anesthetized samples were immediately placed on a plastic dish containing low melting temperature agarose, and positioned at the bottom of the plastic dish. After the agarose set, the dishes were inverted and samples were observed from the flat bottom. Images were acquired using an Olympus SZX16 stereomicroscope with an Olympus E-5 digital camera (Olympus, Tokyo, Japan) under dark-field and oblique light conditions. Anesthetized embryos and larvae were immersed in 4% paraformaldehyde in phosphate buffered saline, rinsed in buffer, and observed under the microscope.

Measurement of Developmental Rate

To find appropriate and suitable experimental conditions for estimation of the developmental rate of goldfish, we first incubated fertilized eggs under five different temperatures (12, 16, 20, 24, and 28°C) by using a gradient temperature incubator TG-5 (FIRSTEC, Taipei, Taiwan). Microscopic observations were conducted at room temperature (22–24°C). We adopted 24°C as the incubation temperature, on account of the stable results obtained, and relative ease of maintaining constant temperature during observation. To estimate developmental timing, fertilized eggs were incubated at 24°C, and early (cleavage and gastrula) and late (segmentation to hatching period) stage embryos were observed at 30 min and 1 hr intervals, respectively. Approximately 10–12 embryos were collected and numbered from one batch of fertilized eggs. Embryo stages were visually inspected and recorded. To increase the accuracy of the developmental time table, observation and recording were repeated in four batches, for a total of 217 points: 2012-04-17-01 (145 points), 2012-04-18-01 (19 points), 2012-04-18-02 (16 points), and 2012-04-25-01 (37 points).

To observe pharyngula and hatching period embryos without exposing embryos repeatedly to room temperature, a separate batch of fertilized eggs were spread onto over 10 plastic Petri dishes. The separately spread embryos were incubated without further manipulation until harvesting. At 24 to 72 hours post fertilization (hpf), embryos and larvae were harvested and anesthetized with MS 222, and then fixed in 4% paraformaldehyde for 1 to 2 hr. Stages were determined, and used to estimate the approximate developmental timing at 24°C (Table 2).

Histology

For detailed observation of tissues and organs, embryos and larvae were harvested and anesthetized with MS 222, fixed in Bouin's fixative, embedded in paraffin, and sectioned at 5 μm. Sliced embryonic sections were stained with hematoxylin and eosin. Larval sections were stained with Alcian blue for visualizing cartilaginous tissues at the hatching stages.

ACKNOWLEDGMENTS

We are grateful to Wen-Hui Su (SHUEN-SHIN Breeding Farm), and You Syu Huang, of the Aquaculture Breeding Institute, Hualien, for technical advice on goldfish breeding in Taiwan. We also thank the following members of the Marine Research Station, Institute of Cellular and Organismic Biology: Hung-Tsai Lee, Cheng-Fu Chang, Jhih-Hao Wei, and Chia-Chun Lee for goldfish maintenance, and Yi-Feei Wang, Shu-Hua Lee, Chi-Fu Hung, and Fei-Chu Chen for administrative support. Finally, we thank Duncan Wright for critical reading of our study.

REFERENCES

Abe G, Ide H, Tamura K. 2007. Function of FGF signaling in the developmental process of the median fin fold in zebrafish. Dev Biol 304:355–366.

Akey JM, Ruhe AL, Akey DT, Wong AK, Connelly CF, Madeoy J, Nicholas TJ, Neff MW. 2010. Tracking footprints of artificial selection in the dog genome. Proc Natl Acad Sci U S A 107:1160–1165.

Albertson RC, Streelman JT, Kocher TD, Yelick PC. 2005. Integration and evolution of the cichlid mandible: the molecular basis of alternate feeding strategies. Proc Natl Acad Sci U S A 102:16287–16292.

Amores A, Force A, Yan Y-L, Joly L, Amemiya C, Fritz A, Ho RK, Langeland J, Prince V, Wang Y-L, Westerfield M, Ekker M, Postlethwait JH. 1998. Zebrafish hox clusters and vertebrate genome evolution. Science 282:1711–1714.

Amsterdam A, Nissen RM, Sun Z, Swindell EC, Farrington S, Hopkins N. 2004. Identification of 315 genes essential for early zebrafish development. Proc Natl Acad Sci U S A 101:12792–12797.

Armstrong PB, Child JS. 1965. Stages in the normal development of Fundulus heteroclitus. Biol Bull 128:143–168.

Asano H, Kubo Y. 1972. Variation of spinal curvature and vertebral number in goldfish. Jpn J Ichthyol 19:233–231.

Ballard WW. 1973. Normal embryonic stages for salmonid fishes, based on Salmo gairdneri Richardson and Salvelinus fontinalis (Mitchill). J Exp Zool 184:7–25.

Bateson W. 1894. Materials for the study of variation: treated with special regard to discontinuity in the origin of species. London: Macmillan.

Battle. 1940. The embryology and larval development of the Goldfish (Carassius auratus L.) from Lake Erie. Ohio J Sci 40:82–93.

Benzie V. 1968. Stages in the normal development of Galaxias maculatus attenuatus (Jenyns). N Z J Mar Freshw 2:606–627.

Bradford Y, Conlin T, Dunn N, Fashena D, Frazer K, Howe DG, Knight J, Mani P, Martin R, Moxon SA, Paddock H, Pich C, Ramachandran S, Ruef BJ, Ruzicka L, Bauer Schaper H, Schaper K, Shao X, Singer A, Sprague J, Sprunger B, Van Slyke C, Westerfield M. 2011. ZFIN: enhancements and updates to the Zebrafish Model Organism Database. Nucleic Acids Res 39:D822–D829.

Carvalho L, Heisenberg CP. 2010. The yolk syncytial layer in early zebrafish development. Trends Cell Biol 20:586–592.

Chan YF, Marks ME, Jones FC, Villarreal G, Shapiro MD, Brady SD, Southwick AM, Absher DM, Grimwood J, Schmutz J, Myers RM, Petrov D, Jónsson B, Schluter D, Bell MA, Kingsley DM. 2010. Adaptive evolution of pelvic reduction in sticklebacks by recurrent deletion of a Pitx1 Enhancer. Science 327:302–305.

Chen J, Tong Y, Zhao S, Ma S, Luo C. 2009. vsx1 3′ untranlated region-mediated translation difference at different developmental stages of goldfish embryos. J Genet Genomics 36:483–490.

Chen SC. 1925. Variation in external characteristics of goldfish Carassius auratus. In: Contributions from the Biological laboratory of the Science Society of China. Shanghai: Science Society of China. p 1–64.

Chen SC. 1956. A history of the domestication and the factors of the varietal formation of the common goldfish, Carassius auratus. Sci Sinica 6:89–116.

Colosimo PF, Peichel CL, Nereng K, Blackman BK, Shapiro MD, Schluter D, Kingsley DM. 2004. The genetic architecture of parallel armor plate reduction in threespine sticklebacks. PLoS Biol 2:e109.

Colosimo PF, Hosemann KE, Balabhadra S, Villarreal G, Dickson M, Grimwood J, Schmutz J, Myers RM, Schluter D, Kingsley DM. 2005. Widespread parallel evolution in sticklebacks by repeated fixation of ectodysplasin Aaleles. Science 307:1928–1933.

Cresko W, McGuigan K, Phillips P, Postlethwait J. 2007. Studies of threespine stickleback developmental evolution: progress and promise. Genetica 129:105–126.

Darwin C, Murray J. 1868. The variation of animals and plants under domestication. London: John Murray.

Davey JW, Hohenlohe PA, Etter PD, Boone JQ, Catchen JM, Blaxter ML. 2011. Genome-wide genetic marker discovery and genotyping using next-generation sequencing. Nat Rev Genet 12:499–510.

Field HA, Dong PDS, Beis D, Stainier DYR. 2003. Formation of the digestive system in zebrafish. ii. pancreas morphogenesis. Dev Biol 261:197–208.

Fujimoto T, Kataoka T, Otani S, Saito T, Aita T, Yamaha E, Arai K. 2004. Embryonic stages from cleavage to gastrula in the loach Misgurnus anguillicaudatus. Zool Sci 21:747–755.

Fujimura K, Okada N. 2007. Development of the embryo, larva and early juvenile of Nile tilapia Oreochromis niloticus (Pisces: Cichlidae). developmental staging system. Dev Growth Differ 49:301–324.

Gilbert SF. 2010. Developmental biology. Sunderland: Sinauer Associates, Inc.

Gross JM, Perkins BD, Amsterdam A, Egana A, Darland T, Matsui JI, Sciascia S, Hopkins N, Dowling JE. 2005. Identification of zebrafish insertional mutants with defects in visual system development and function. Genetics 170:245–261.

Hall TE, Smith P, Johnston IA. 2004. Stages of embryonic development in the Atlantic cod Gadus morhua. J Morphol 259:255–270.

Hammerschmidt M, Pelegri F, Mullins MC, Kane DA, van Eeden FJ, Granato M, Brand M, Furutani-Seiki M, Haffter P, Heisenberg CP, Jiang YJ, Kelsh RN, Odenthal J, Warga RM, Nusslein-Volhard C. 1996. dino and mercedes, two genes regulating dorsal development in the zebrafish embryo. Development 123:95–102.

Hervey GF, Hems J. 1948. The Goldfish. London: Batchworth Press.

Hinaux H, Pottin K, Chalhoub H, Pere S, Elipot Y, Legendre L, Retaux S. 2011. A developmental staging table for Astyanax mexicanus surface fish and pachón cavefish. Zebrafish 8:155–165.

Hoegg S, Brinkmann H, Taylor J, Meyer A. 2004. Phylogenetic timing of the fish-specific genome duplication correlates with the diversification of teleost fish. J Mol Evol 59:190–203.

Holland PW, Garcia-Fernàndez J. 1996. Hox genes and chordate evolution. Dev Biol 173:382–395.

Iwamatsu T. 2004. Stages of normal development in the medaka Oryzias latipes. Mech Dev 121:605–618.

Jaillon O, Aury J-M, Brunet F, Petit J-L, Stange-Thomann N, Mauceli E, Bouneau L, Fischer C, Ozouf-Costaz C, Bernot A, Nicaud S, Jaffe D, Fisher S, Lutfalla G, Dossat C, Segurens B, Dasilva C, Salanoubat M, Levy M, Boudet N, Castellano S, Anthouard V, Jubin C, Castelli V, Katinka M, Vacherie B, Biemont C, Skalli Z, Cattolico L, Poulain J, de Berardinis V, Cruaud C, Duprat S, Brottier P, Coutanceau J-P, Gouzy J, Parra G, Lardier G, Chapple C, McKernan KJ, McEwan P, Bosak S, Kellis M, Volff J-N, Guigo R, Zody MC, Mesirov J, Lindblad-Toh K, Birren B, Nusbaum C, Kahn D, Robinson-Rechavi M, Laudet V, Schachter V, Quetier F, Saurin W, Scarpelli C, Wincker P, Lander ES, Weissenbach J, Roest Crollius H. 2004. Genome duplication in the teleost fish Tetraodon nigroviridis reveals the early vertebrate proto-karyotype. Nature 431:946–957.

Jeffery WR. 2001. Cavefish as a model system in evolutionary developmental biology. Dev Biol 231:1–12.

Ishida J. 1985. Hatching enzyme: past, present and future. Zool Sci 2:1–10.

Kajishima T. 1960. The normal developmental stages of the goldfish Carassius auratus. Jpn J Ichthyol 8:20–28.

Kanki JP, Ho RK. 1997. The development of the posterior body in zebrafish. Development 124:881–893.

Keller RE, Danilchik M, Gimlich R, Shih J. 1985. The function and mechanism of convergent extension during gastrulation of Xenopus laevis. J Embryol Exp Morphol 89:185–209.

Khan MH. 1929. Early stages in the development of the goldfish (Carassius auratus). J Bombay Nat Hist Soc 33:614–617.

Kim SK, Shindo A, Park TJ, Oh EC, Ghosh S, Gray RS, Lewis RA, Johnson CA, Attie-Bittach T, Katsanis N, Wallingford JB. 2010. Planar cell polarity acts through septins to control collective cell movement and ciliogenesis. Science 329:1337–1340.

Kimmel CB, Kane DA, Walker C, Warga RM, Rothman MB. 1989. A mutation that changes cell-movement and cell fate in the zebrafish embryo. Nature 337:358–362.

Kimmel CB, Ballard WW, Kimmel SR, Ullmann B, Schilling TF. 1995. Stages of embryonic development of the zebrafish. Dev Dyn 203:253–310.

Kimmel CB, Ullmann B, Walker C, Wilson C, Currey M, Phillips PC, Bell MA, Postlethwait JH, Cresko WA. 2005. Evolution and development of facial bone morphology in threespine sticklebacks. Proc Natl Acad Sci U S A 102: 5791–5796.

Kitano J, Bolnick DI, Beauchamp DA, Mazur MM, Mori S, Nakano T, Peichel CL. 2008. Reverse evolution of armor plates in the threespine stickleback. Curr Biol 18:769–774.

Koh T-P. 1931. Osteology of Carassius auratus. Science report national Ts'ing Hua University 1:61–81.

Koh T-P. 1932. Osteological variations in the axial skeleton of goldfish (Carassius auratus). Science report national Ts'ing Hua University 2:109–121.

Komiyama T, Kobayashi H, Tateno Y, Inoko H, Gojobori T, Ikeo K. 2009. An evolutionary origin and selection process of goldfish. Gene 430:5–11.

Latimer A, Jessen JR. 2010. Extracellular matrix assembly and organization during zebrafish gastrulation. Matrix Biol 29:89–96.

Larhammar D, Risinger C. 1994. Molecular genetic aspects of tetraploidy in the common carp Cyprinus carpio. Mol Phylogenet Evol 3:59–68.

le Pabic P, Stellwag EJ, Scemama J-L. 2009. Embryonic development and skeletogenesis of the pharyngeal jaw apparatus in the cichlid nile tilapia (Oreochromis niloticus). Anat Rec 292: 1780–1800.

Lindblad-Toh K, Wade CM, Mikkelsen TS, Karlsson EK, Jaffe DB, Kamal M, Clamp M, Chang JL, Kulbokas EJ, 3rd, Zody MC, Mauceli E, Xie X, Breen M, Wayne RK, Ostrander EA, Ponting CP, Galibert F, Smith DR, DeJong PJ, Kirkness E, Alvarez P, Biagi T, Brockman W, Butler J, Chin CW, Cook A, Cuff J, Daly MJ, DeCaprio D, Gnerre S, Grabherr M, Kellis M, Kleber M, Bardeleben C, Goodstadt L, Heger A, Hitte C, Kim L, Koepfli KP, Parker HG, Pollinger JP, Searle SM, Sutter NB, Thomas R, Webber C, Baldwin J, Abebe A, Abouelleil A, Aftuck L, Ait-Zahra M, Aldredge T, Allen N, An P, Anderson S, Antoine C, Arachchi H, Aslam A, Ayotte L, Bachantsang P, Barry A, Bayul T, Benamara M, Berlin A, Bessette D, Blitshteyn B, Bloom T, Blye J, Boguslavskiy L, Bonnet C, Boukhgalter B, Brown A, Cahill P, Calixte N, Camarata J, Cheshatsang Y, Chu J, Citroen M, Collymore A, Cooke P, Dawoe T, Daza R, Decktor K, DeGray S, Dhargay N, Dooley K, Dorje P, Dorjee K, Dorris L, Duffey N, Dupes A, Egbiremolen O, Elong R, Falk J, Farina A, Faro S, Ferguson D, Ferreira P, Fisher S, FitzGerald M, Foley K, Foley C, Franke A, Friedrich D, Gage D, Garber M, Gearin G, Giannoukos G, Goode T, Goyette A, Graham J, Grandbois E, Gyaltsen K, Hafez N, Hagopian D, Hagos B, Hall J, Healy C, Hegarty R, Honan T, Horn A, Houde N, Hughes L, Hunnicutt L, Husby M, Jester B, Jones C, Kamat A, Kanga B, Kells C, Khazanovich D, Kieu AC, Kisner P, Kumar M, Lance K, Landers T, Lara M, Lee W, Leger JP, Lennon N, Leuper L, LeVine S, Liu J, Liu X, Lokyitsang Y, Lokyitsang T, Lui A, Macdonald J, Major J, Marabella R, Maru K, Matthews C, McDonough S, Mehta T, Meldrim J, Melnikov A, Meneus L, Mihalev A, Mihova T, Miller K, Mittelman R, Mlenga V, Mulrain L, Munson G, Navidi A, Naylor J, Nguyen

T, Nguyen N, Nguyen C, Nicol R, Norbu N, Norbu C, Novod N, Nyima T, Olandt P, O'Neill B, O'Neill K, Osman S, Oyono L, Patti C, Perrin D, Phunkhang P, Pierre F, Priest M, Rachupka A, Raghuraman S, Rameau R, Ray V, Raymond C, Rege F, Rise C, Rogers J, Rogov P, Sahalie J, Settipalli S, Sharpe T, Shea T, Sheehan M, Sherpa N, Shi J, Shih D, Sloan J, Smith C, Sparrow T, Stalker J, Stange-Thomann N, Stavropoulos S, Stone C, Stone S, Sykes S, Tchuinga P, Tenzing P, Tesfaye S, Thoulutsang D, Thoulutsang Y, Topham K, Topping I, Tsamla T, Vassiliev H, Venkataraman V, Vo A, Wangchuk T, Wangdi T, Weiand M, Wilkinson J, Wilson A, Yadav S, Yang S, Yang X, Young G, Yu Q, Zainoun J, Zembek L, Zimmer A, Lander ES. 2005. Genome sequence, comparative analysis and haplotype structure of the domestic dog. Nature 438:803–819.

Li P, Wang AQ, Cui DF, Mou GY, Wang CY, Zhang RQ, Ning YH, Zhang NC. 1959. Normal stages in the development of wild and domesticated goldfish. Carassius auratus. Acta Zool Sin 11: 145–154.

Luo J, Lang M, Salzburger W, Siegel N, Stolting KN, Meyer A. 2006. A BAC library for the goldfish Carassius auratus auratus (Cyprinidae, Cypriniformes). J Exp Zool Part B Mol Dev Evol 306B:567–574.

Magyary I, Urbanyi B, Horváth L. 1996. Cryopreservation of common carp (Cyprinus carpio L.) sperm II. Optimal conditions for fertilization. J Appl Ichthyol 12:117–119.

Martinez GM, Bolker JA. 2003. Embryonic and larval staging of summer flounder (Paralichthys dentatus). J Morphol 255:162–176.

Matsui Y. 1934. Genetical studies on goldfish of Japan. J Imp Fish Inst 30:1–96.

Matsui Y, Axelrod HR. 1991. Goldfish guide. Neptune City: T.F.H. Publications, Inc.

Meyer A, Van de Peer Y. 2005. From 2R to 3R: evidence for a fish-specific genome duplication (FSGD). Bioessays 27:937–945.

Metzker ML. 2010. Sequencing technologies – the next generation. Nat Rev Genet 11:31–46.

Mizuno T, Yamaha E, Yamazaki F. 1997. Localized axis determinant in the early cleavage embryo of the goldfish, Carassius auratus. Dev Genes Evol 206:389–396.

Mizuno T, Yamaha E, Kuroiwa A, Takeda H. 1999. Removal of vegetal yolk causes dorsal deficiencies and impairs dorsal-inducing ability of the yolk cell in zebrafish. Mech Dev 81:51–63.

Morey DF. 1994. The early evolution of the domestic dog. Am Sci 82:336–347.

Mullins MC, Hammerschmidt M, Haffter P, Nusslein-Volhard C. 1994. Large-scale mutagenesis in the zebrafish: in search of genes controlling development in a vertebrate. Curr Biol 4:189–202.

Mullins MC, Hammerschmidt M, Kane DA, Odenthal J, Brand M, van Eeden FJ, Furutani-Seiki M, Granato M, Haffter P, Heisenberg CP, Jiang YJ, Kelsh RN, Nusslein-Volhard C. 1996. Genes establishing dorsoventral pattern formation in the zebrafish embryo: the ventral specifying genes. Development 123:81–93.

Nagai T, Yamaha E, Arai K. 2001. Histological differentiation of primordial germ cells in zebrafish. Zool Sci 18:215–223.

Neuhauss SC, Solnica-Krezel L, Schier AF, Zwartkruis F, Stemple DL, Malicki J, Abdelilah S, Stainier DY, Driever W. 1996. Mutations affecting craniofacial development in zebrafish. Development 123:357–367.

Ng ANY, de Jong-Curtain TA, Mawdsley DJ, White SJ, Shin J, Appel B, Dong PDS, Stainier DYR, Heath JK. 2005. Formation of the digestive system in zebrafish: III. Intestinal epithelium morphogenesis. Dev Biol 286:114–135.

Ohno S, Wolf U, Atkin NB. 1968. Evolution from fish to mammals by gene duplication. Heredity 59:169–187.

Ojima Y. 1983. Fish cytogenetics. Tokyo: Suiko–sha.

Otani S, Maegawa S, Inoue K, Arai K, Yamaha E. 2002. The germ cell lineage identified by vas-mRNA during the embryogenesis in goldfish. Zool Sci 19: 519–526.

Ouji M. 1955. Morphology and development of the hatching glands of the teleost, Cyprinus auratus. Zoological magazine; Dobutsugaku zasshi 64:277–279.

Parichy DM, Elizondo MR, Mills MG, Gordon TN, Engeszer RE. 2009. Normal table of postembryonic zebrafish development: staging by externally visible anatomy of the living fish. Dev Dyn 238:2975–3015.

Passini MA, Levine EM, Canger AK, Raymond PA, Schechter N. 1997. Vsx-1 and Vsx-2: Differential expression of two Paired-like homeobox genes during zebrafish and goldfish retinogenesis. J Comp Neurol 388:495–505.

Peichel CL, Nereng KS, Ohgi KA, Cole BLE, Colosimo PF, Buerkle CA, Schluter D, Kingsley DM. 2001. The genetic architecture of divergence between threespine stickleback species. Nature 414:901–905.

Reib JP. 1973. La circulation sanguine chez l'embryon de Brachydanio rerio. Ann Embryol Morphol 6:43–54.

Risinger C, Larhammar D. 1993. Multiple loci for synapse protein SNAP-25 in the tetraploid goldfish. Proc Natl Acad Sci U S A 90:10598–10602.

Rohde LA, Heisenberg CP. 2007. Zebrafish gastrulation: cell movements, signals, and mechanisms. Int Rev Cytol 261:159–192.

Rohner N, Bercsènyi M, Orban L, Kolanczyk ME, Linke D, Brand M, Nusslein-Volhard C, Harris MP. 2009. Duplication of fgfr1 Permits Fgf signaling to serve as a target for selection during domestication. Curr Biol 19: 1642–1647.

Saitoh K, Miya M, Inoue JG, Ishiguro NB, Nishida M. 2003. Mitochondrial genomics of ostariophysan fishes: perspectives on phylogeny and biogeography. J Mol Evol 56:464–472.

Saitoh K, Sado T, Mayden RL, Hanzawa N, Nakamura K, Nishida M, Miya M. 2006. Mitogenomic evolution and interrelationships of the Cypriniformes (Actinopterygii: Ostariophysi): the first evidence toward resolution of higher-level relationships of the world's largest freshwater fish clade based on 59 whole mitogenome sequences. J Mol Evol 63: 826–841.

Sato Y, Nishida M. 2010. Teleost fish with specific genome duplication as unique models of vertebrate evolution. Environ Biol Fish 88:169–188.

Schilling TF, Kimmel CB. 1997. Musculoskeletal patterning in the pharyngeal segments of the zebrafish embryo. Development 124:2945–2960.

Sèmon M, Wolfe KH. 2007. Consequences of genome duplication. Curr Opin Genet Dev 17:505–512.

Shapiro MD, Kronenberg Z, Li C, Domyan ET, Pan H, Campbell M, Tan H, Huff CD, Hu H, Vickrey AI, Nielsen SC, Stringham SA, Willerslev E, Gilbert MT, Yandell M, Zhang G, Wang J. 2013. Genomic diversity and evolution of the head crest in the rock pigeon. Science 339:1063–1067.

Sharma SC, Ungar F. 1980. Histogenesis of the goldfish retina. J Comp Neurol 191:373–382.

Smartt J. 2001. Goldfish varieties and genetics: a handbook for breeders. Malden, MA: Blackwell Science.

Stainier DYR, Fishman MC. 1992. Patterning the zebrafish heart tube: acquisition of anteroposterior polarity. Dev Biol 153:91–101.

Stringham Sydney A, Mulroy Elisabeth E, Xing J, Record D, Guernsey Michael W, Aldenhoven Jaclyn T, Osborne Edward J, Shapiro Michael D. 2012. Divergence, convergence, and the ancestry of feral populations in the domestic rock pigeon. Curr Biol 22:302–308.

Swarup H. 1958. Stages in the development of the stickleback Gasterosteus aculeatus (L.). J Embryol Exp Morphol 6:373–383.

Takeda H, Shimada A. 2010. The art of medaka genetics and genomics: what makes them so unique? Annu Rev Genet 44:217–241.

Tanaka M, Yamaha E, Arai K. 2004. Survival capacity of haploid-diploid goldfish chimeras. J Exp Zool A 301A:491–501.

Trut L, Oskina I, Kharlamova A. 2009. Animal evolution during domestication: the domesticated fox as a model. Bioessays 31:349–360.

vanEeden FJ, Granato M, Schach U, Brand M, Furutani-Seiki M, Haffter P, Hammerschmidt M, Heisenberg CP, Jiang YJ, Kane DA, Kelsh RN, Mullins MC, Odenthal J, Warga RM, Allende ML, Weinberg ES, Nusslein-Volhard C. 1996a. Mutations affecting somite

formation and patterning in the zebrafish, Danio rerio. Development 123:153–164.

vanEeden FJM, Granato M, Schach U, Brand M, FurutaniSeiki M, Haffter P, Hammerschmidt M, Heisenberg CP, Jiang YJ, Kane DA, Kelsh RN, Mullins MC, Odenthal J, Warga RM, NussleinVolhard C. 1996b. Genetic analysis of fin formation in the zebrafish, Danio rerio. Development 123:255–262.

VonHoldt BM, Pollinger JP, Lohmueller KE, Han E, Parker HG, Quignon P, Degenhardt JD, Boyko AR, Earl DA, Auton A, Reynolds A, Bryc K, Brisbin A, Knowles JC, Mosher DS, Spady TC, Elkahloun A, Geffen E, Pilot M, Jedrzejewski W, Greco C, Randi E, Bannasch D, Wilton A, Shearman J, Musiani M, Cargill M, Jones PG, Qian Z, Huang W, Ding ZL, Zhang YP, Bustamante CD, Ostrander EA, Novembre J, Wayne RK. 2010. Genome-wide SNP and haplotype analyses reveal a rich history underlying dog domestication. Nature 464:898–902.

Watase S. 1887. On the caudal and anal fins of goldfishes. Journal of the Science Colleage, Imperial University, Tokyo, Japan 1:247–267.

Wayne RK, Ostrander EA. 2007. Lessons learned from the dog genome. Trends Genet 23:557–567.

Westerfield M. 2000. The zebrafish book. A guide for the laboratory use of zebrafish (Danio rerio). Eugene: University of Oregon Press.

Yamaha E, Yamazaki F. 1993. Electrically fused-egg induction and its development in the goldfish, Carassius auratus. Int J Dev Biol 37:291–298.

Yamaha E, Mizuno T, Hasebe Y, Takeda H, Yamazaki F. 1998. Dorsal specification in blastoderm at the blastula stage in the goldfish, Carassius auratus. Dev Growth Differ 40:267–275.

Yamaha E, Mizuno T, Matsushita K, Hasebe Y. 1999. Developmental staging in goldfish during the pre-gastula stage. Nippon Suisan Gakkaishi 65:709–717.

Yamaha E, Kazama-Wakabayashi M, Otani S, Fujimoto T, Arai K. 2001. Germ-line chimera by lower-part blastoderm transplantation between diploid goldfish and triploid crucian carp. Genetica 111:227–236.

Yamaha E, Otani S, Minami A, Arai K. 2002. Dorso-ventral axis perturbation in goldfish embryos caused by heat- and pressure-shock treatments for chromosome set manipulation. Fish Sci 68:313–319.

Yamaha E, Murakami M, Hada K, Otani S, Fujimoto T, Tanaka M, Sakao S, Kimura S, Sato S, Arai K. 2003. Recovery of fertility in male hybrids of a cross between goldfish and common carp by transplantation of PGC (Primordial Germ Cell)-containing graft. Genetica 119:121–131.

Yamamoto Y, Jeffery WR. 2000. Central role for the lens in cave fish eye degeneration. Science 289:631–633.

Yamamoto Y, Stock DW, Jeffery WR. 2004. Hedgehog signalling controls eye degeneration in blind cavefish. Nature 431:844–847.

Yamamoto Y, Byerly MS, Jackman WR, Jeffery WR. 2009. Pleiotropic functions of embryonic sonic hedgehog expression link jaw and taste bud amplification with eye loss during cavefish evolution. Dev Biol 330:200–211.

Yang L, Gui J-F. 2004. Positive selection on multiple antique allelic lineages of transferrin in the polyploid Carassius auratus. Mol Biol Evol 21:1264–1277.

Yano T, Tamura K. 2013. The making of differences between fins and limbs. J Anat 222:100–113.

Zhong TP. 2005. Zebrafish genetics and formation of embryonic vasculature. In: Gerald PS, editor. Curr Top Dev Biol 71:53–81.

Developmental Dynamics